



Analysis of post-fire suspended sediment sources by using colour parameters

Julián García-Comendador^{a,b,*}, Núria Martínez-Carreras^c, Josep Fortesa^{a,b}, Antoni Borràs^d,
Aleix Calsamiglia^{a,b}, Joan Estrany^{a,b}

^a Mediterranean Ecogeomorphological and Hydrological Connectivity Research Team (<http://medhycon.uib.cat>), Department of Geography, University of the Balearic Islands, Carretera de Valldemossa Km 7.5, 07122 Palma, Balearic Islands, Spain

^b Institute of Agro-Environmental and Water Economy Research –INAGEA (<http://inagea.com/>), University of the Balearic Islands, Carretera de Valldemossa Km 7.5, 07122 Palma, Balearic Islands, Spain

^c Catchment and Eco-Hydrology Research Group (CAT), Environmental Research and Innovation Department (ERIN), Luxembourg Institute of Science and Technology (LIST), 41, Rue du Brill, L-4422 Belvaux, Luxembourg

^d Environmental Radioactivity Laboratory (<https://labora.uib.es/>), Department of Physics, University of the Balearic Islands, Carretera de Valldemossa Km 7.5, 07122 Palma, Balearic Islands, Spain

ARTICLE INFO

Handling editor: Cathelijne Stoof

Keywords:

Sediment fingerprinting

Colour

Fallout radionuclides

Wildfire

Ash

Suspended sediment sources

ABSTRACT

After a wildfire, total or partial removal of vegetal biomass and changes in physicochemical soil properties lead to an increase in overland flow and sediment yield. Eventual damage must be counteracted urgently by identifying erosion hotspots and by implementing post-fire management programmes and sampling campaigns. In this context, the sediment source fingerprinting technique is widely used to determine the origin of suspended sediments in catchments and to evaluate the effectiveness of sediment management programmes. It traditionally relies on the use of physical, biochemical and geochemical properties as tracers. However, measuring these tracers in the laboratory is often expensive and time-consuming. Colour tracers have been shown to greatly reduce time and cost, especially if a normal office scanner is used for measurements. Here we explored whether colour parameters can be used to investigate suspended sediment origin in burned catchments. To this end, sediment and ash were mixed artificially to verify colour linear additivity and ash influence on colour parameters. Colour parameters were then used for source ascription of suspended sediment samples ($n = 9$) collected during two years after a fire in a small Mediterranean catchment (Mallorca, Spain). In addition, reflectance-derived colour parameters were compared with those obtained using a normal office scanner. The close correlation between most chromatic indexes (obtained using both methods; $p < 0.01$) suggested that scanning is a good alternative for measuring soil and sediment colour. A Bayesian tracer mixing model (MixSIAR) determined the relative contribution of each source. The type of mixing model enables appropriate representation of natural and sampling uncertainty in tracer data. During the first events, suspended sediment originated mainly in burned surfaces, whereas the contribution of these decreased throughout the study period. Tracing results obtained using colour parameters were compared with calculations using ^{137}Cs and $^{210}\text{Pb}_{\text{ex}}$ as recognized tracers to discriminate between surface and subsurface sediment sources after wildfires. Estimated source ascriptions with both methods (i.e. reflectance-derived colour parameters and radionuclides) coincided in predicting the dominant source in 7 of the 9 samples measured. Colour tracers proved useful in discriminating between burned and unburned sources, making them suitable for suspended sediment source ascription and monitoring as part of post-fire management strategies.

1. Introduction

Wildfires greatly change the hydrological response and sediment dynamics of river systems (Moody et al., 2013; Shakesby, 2011; Shakesby and Doer, 2006). The reduction or elimination of vegetation

cover (Candela et al., 2005) and the alteration of physicochemical soil characteristics (Úbeda and Outeiro, 2009) normally increase overland flow and sediment yield from hillslopes and reduce the rainfall-runoff response time, especially during the first post-fire year (Candela et al., 2005; Scott et al., 1998). Other variables that affect the increase in

* Corresponding author at: Mediterranean Ecogeomorphological and Hydrological Connectivity Research Team (<http://medhycon.uib.cat>), Department of Geography, University of the Balearic Islands, Carretera de Valldemossa Km 7.5, 07122 Palma, Balearic Islands, Spain.

E-mail address: julian.garcia@uib.cat (J. García-Comendador).

<https://doi.org/10.1016/j.geoderma.2020.114638>

Received 9 May 2020; Received in revised form 20 July 2020; Accepted 28 July 2020

Available online 05 August 2020

0016-7061/ © 2020 Elsevier B.V. All rights reserved.

erosion and sediment yield after a fire are the fire's severity (Keeley, 2009), post-fire rainfall patterns (Warrick et al., 2012), lithology and the presence of agricultural terraces (García-Comendador et al., 2017a), and post-fire management (Spanos et al., 2005). In addition, the increase in slope-to-channel sediment connectivity may generate downstream impacts related to fine sediment transport and its associated pollutants (Collins et al., 2017), such as dam siltation (Navas et al., 2004), decreased water quality (Horowitz et al., 2007; Smith et al., 2011a) and the contamination of aquatic ecosystems (Newcombe and Macdonald, 1991; Verkaik et al., 2013).

Fire transforms biomass, necromass and soil organic matter into ash, consisting of mineral materials and charred organic components (Bodí et al., 2014). A non-homogenous ash layer covers the soil surface immediately after a wildfire creating a two-layer system (Nyman et al., 2014), influencing soil wettability (Balfour and Woods, 2013; Bodí et al., 2014; Cerdà and Doerr, 2008) and altering its hydrological behaviour (Brook et al., 2018). Nevertheless, ash does not remain on the soil surface for very long, but is redistributed or removed in days or weeks after a fire (Cerdà and Doerr, 2008; Pereira et al., 2015), is transported in the river in combination with fine sediment (Reneau et al., 2007) and/or migrates downward into the soil (Pereira et al., 2015). However, little is known about how ash reaches the stream network after a fire and its progressive wash-out as suspended sediment, as this process is highly dependent on ash properties, terrain features and meteorological conditions (Bodí et al., 2014). Accurate identification of the suspended sediment sources contributing to sediment load after a wildfire and of routine monitoring programmes are needed to correctly design and evaluate post-fire management strategies, which are crucial in fire-prone, human-modified environments.

In river catchments, fingerprinting and unmixing techniques are often used to calculate the different pre-defined sources in a downstream suspended sediment mixture (Davis and Fox, 2009; Walling et al., 1993). Traditionally, physical, biochemical and geochemical sediment properties are used as tracers (Walling, 2013). Sediment fingerprinting assumes that tracer properties are measurable, conservative and representative, which needs to be carefully scrutinized (Collins et al., 2017; Smith and Blake, 2014). In addition, the tracers must behave in a linearly additive way during the mixing process (Lees, 1997). Previous studies have shown that the use of some of these tracers is not appropriate in burned catchments. For example, susceptibility to the variation of soil geochemical properties after a fire hinders the distinction between burned and unburned areas (Smith et al., 2013). On the contrary, the fallout radionuclides (FRNs), caesium-137 (^{137}Cs) and excess lead-210 ($^{210}\text{Pb}_{\text{ex}}$), normally increase their activity in soils after a wildfire due to soil mass reduction by organic matter combustion and to radionuclide transfer and redistribution from burned vegetation to the soil (Wilkinson et al., 2009), which discriminates between burned and unburned areas (Estrany et al., 2016; García-Comendador et al., 2017b). In addition, their exposure to atmospheric precipitation discriminates between surface and subsurface sources (Owens et al., 2012; Wilkinson et al., 2009), which has led to their extensive use in burned catchments. However, catchment vulnerability to erosion processes during the first post-fire year highlights the need to define and apply cost-effective and fast post-fire management strategies, whereas FRN counting times in samples with relatively low activity are rather long.

Soil and sediment colour can also be used for tracing, the main advantage being that this can be measured by fast, cheap and non-destructive methods. Colour coefficients use as tracers for source ascription has increased in the last decade (Evrard et al., 2019; Martínez-Carreras et al., 2010b; Pulley et al., 2018; Tiecher et al., 2015), as the results obtained were found to be comparable to those obtained with classical tracers (i.e. radionuclides, geochemistry and organic compounds) in small catchments (Martínez-Carreras et al., 2010a,c). Pulley et al. (2018) found high consistency between estimates based on mineral magnetic tracers and ones based on colour coefficients in clarifying the sediment sources of historically deposited sediments.

However, special attention should be paid to how changes in organic matter content, particle size distribution and moisture alter colour properties (Pulley and Rowntree, 2016). These parameters may affect the probabilistic distributions calculated by mixing models, which may in turn lead to wrong conclusions. Nonetheless, the elimination of organic matter or the use of particle size correction factors may not be suitable in all cases and may even reduce the discriminative potential of colour tracers (Pulley et al., 2018; Pulley and Rowntree, 2016).

Previous studies used ash colour (Úbeda et al., 2009) and changes in soil colour (D'Haen et al., 2013; Ketterings and Bigham, 2000; Pérez-Bejarano and Guerrero, 2018) to determine the temperature reached during a fire. Normally, black ashes appear at low temperatures (ca. 250 °C) because of the residual carbon content derived from the incomplete combustion of the organic matter; and grey ashes, at temperatures above ca. 450 °C due to the mineral residue after complete combustion (Lentile et al., 2006; Smith et al., 2005; Úbeda et al., 2009). The presence of black ash after fire tends to decrease visible and near-infrared reflectance. In contrast, the silica mineral present in grey ash tends to increase it greatly (Lentile et al., 2006). Furthermore, soil tends to become redder when temperature reaches a range between 200 and 500 °C. This is due to the transformation of iron oxides hydrated first into maghemite and then hematite (Terefe et al., 2008). These features help to distinguish sediment origin when using colour tracers after a fire.

This paper puts forward the proposition that suspended sediment colour shows the relative contributions of burned and unburned surfaces in river catchments. Artificial mixtures of sediment and ash were created to verify linear additivity and ash influence on colour parameters. Suspended sediment tracing results obtained by colour parameters calculated from reflectance diffuse spectrometry were compared, in order to investigate the sediment's consistency, with those obtained (i) using an ordinary office scanner and (ii) fallout radionuclides.

2. Study area

The Sa Font de la Vila River is a Mediterranean catchment of 4.8 km² located in the Andratx municipality (western Mallorca, Spain; Fig. 1A and 1B), which is affected by extensive afforestation of former agricultural land and recurrent wildfires. The lithology of the catchment's bottom valleys consists mainly of Upper Triassic (Keuper) clays and loams on gentle slopes (ca. < 10°). Rhaetian dolomite and Lias limestone predominate in the upper parts of the catchment with steeper slopes > 30% (Fig. 1c). Soils are classified as *BK45-2bc*, corresponding to *Calcic Cambisols* (Jahn et al., 2006). The fluvial network consists of two main streams: (a) Sa Coma Freda (east, 2.3 km²), which has a significant groundwater influence with several karstic springs; and (b) Can Cabrit (west, 2.08 km²), not affected by this groundwater influence due to the reduced presence of impervious materials. In addition, a check-dam was built at Can Cabrit in 2007 (5 m high and 16 m long; Fig. 1D).

The climate is Mediterranean temperate sub-humid at headwaters and warm sub-humid at the outlet (Emberger climatic classification; Guijarro, 1986). The average temperature is 16.5 °C. The mean annual rainfall is 518 mm yr⁻¹, with an inter-annual coefficient of variation of 29%. High-intensity rainstorms with a recurrence period of 10 years may reach 85 mm in 24 h (1974–2010; data from the B118 S'Alqueria meteorological station of the Spanish State Meteorological Agency (AEMET); Fig. 1B).

In the last twenty years, the Sa Font de la Vila catchment has been affected by major wildfires in 1994 and 2013 (Fig. 1E). Before the 2013 wildfire, the catchment was mainly covered by natural vegetation (84%; Fig. 1C): 51% forest and 33% scrubland. The rest of the catchment was covered by rain-fed tree crops (12%), rain-fed herbaceous crops (1%) and urban uses (3%). Traditional soil and water conservation structures (i.e., hillslope and valley-bottom terraces) cover 37% of

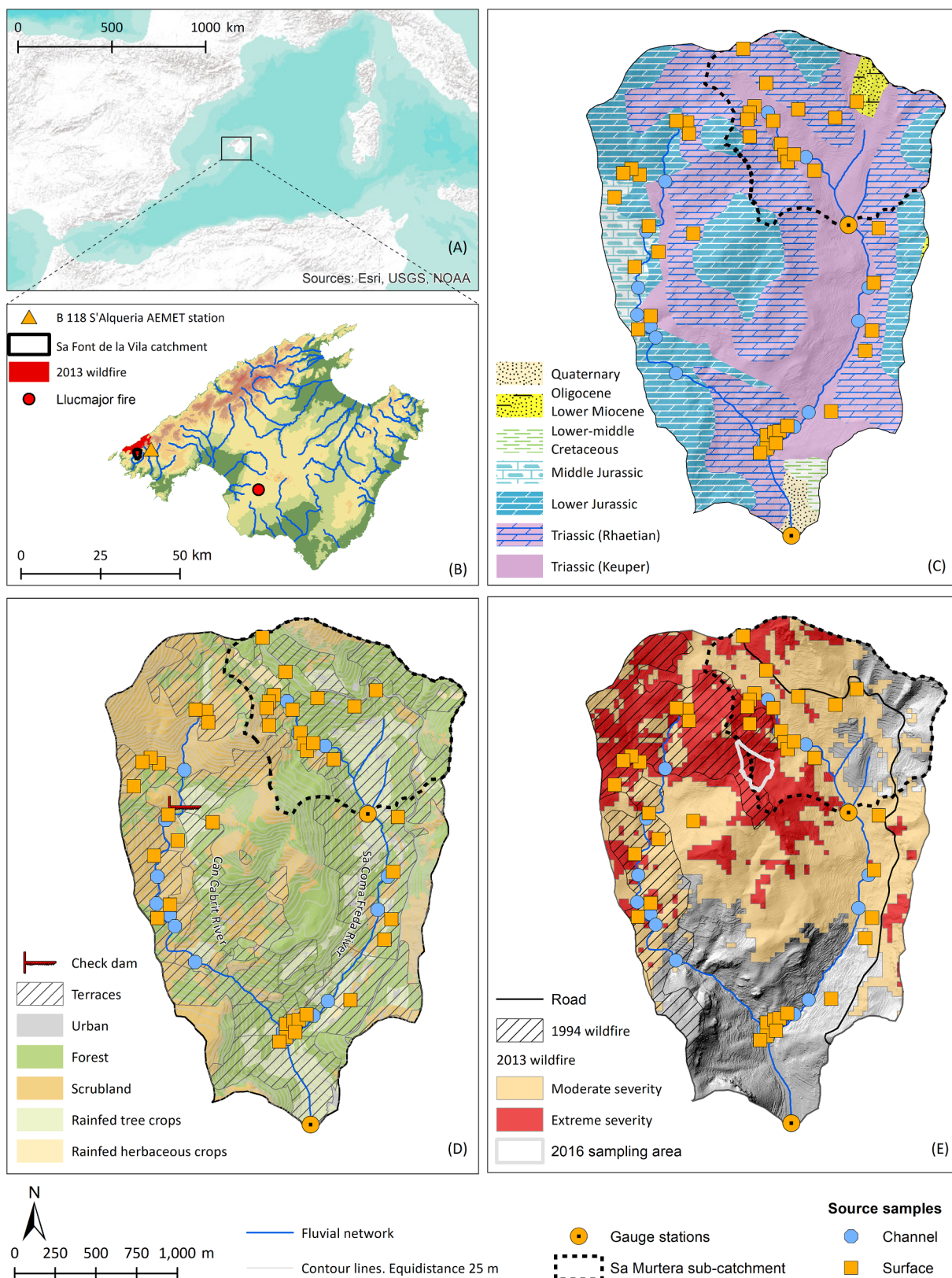


Fig. 1. Location of the Mallorca Island within the Mediterranean Sea (A); location of the Sa Font de la Vila catchment, the area affected by the July 2013 wildfire, the B'12 S'Alqueria meteorological station and the village of Lluçmajor (B); lithology (C) land uses and soil conservation practices (D) of the Sa Font de la Vila catchment (*downstream site*) and Sa Murtera sub-catchment (*upstream site*); and 1994 and 2013 wildfire affected areas as well as severity of the 2013 wildfire and 2016 sampling area (E). Channel bank and surface sampling points indicated as blue dots and orange squares, respectively.

the total surface area (Fig. 1D). Their abandonment and degradation, involving the collapse of dry-stone walls, increased the sensitivity of the catchment (Calsamiglia et al., 2017). Collapses were higher on those abandoned terraces affected by recurrent fires due to soil degradation (Lucas-Borja et al., 2018).

The 1994 fire affected 45% of the catchment surface, whereas the 2013 one reached 71% (more than half of it had already been burned in 1994). A severity assessment with the Normalized Burn Ratio (Escuin et al., 2008) and Landsat 8 images for the 2013 wildfire assigned high and moderate severity to 24% and 47% of the catchment, respectively (Bauzá, 2014, Fig. 1E). In addition, after the 2013 wildfire the Balearic Islands Department of the Environment (Conselleria de Medi Ambient, Agricultura i Pesca) implemented a series of post-fire strategies to prevent soil loss and degradation, which included mulching, tree planting and the creation of log barriers with dead biomass.

3. Materials and methods

3.1. Water and sediment monitoring programme

Two nested gauging stations were installed in Sa Font de la Vila catchment to record continuous water and suspended sediment fluxes, one at the Sa Murtera sub-catchment (1.1 km²; *upstream site*) and one at the outlet of the catchment (4.8 km²; *downstream site*; Fig. 1). As the *upstream site* gauging station was not set up till September 2014, hydrological data are not available for the first post-fire year. Both stations were equipped with *Campbell Scientific CS451-L* pressure probes and *OBS-3* + turbidimeters with a double measurement range of 0–1,000 and 1,000–4,000 NTU. *Campbell CR200* loggers recorded 15-min average values of water stage and turbidity (based on 1-minute readings). In addition, a *Casella* tipping bucket rain gauge was installed at the *upstream site*.

3.2. Soil, ash and sediment sampling

After careful examination of the site, samples of potential sediment sources were collected immediately after the last wildfire (September 2013; Fig. 1) on soil hillslopes with an apparently active sediment slope-to-channel connectivity (0–2 cm depth; n = 40) and potential erodible channel banks (n = 20). To encompass the spatial variability of the soil properties, each surface soil sample consisted of three integrated subsamples collected inside a ca. 10 m-radius circular area; and each channel bank sample, of three subsamples collected along a 10 m transect. The fire impact was taken into account when designing the surface sample collection strategy. Thirty-one surface samples were collected from burned areas (burned surface samples) and 9 from unburned areas (unburned surface samples; Fig. 1E). For the *upstream site* only 4 channel bank samples and 15 burned surface samples were collected. The unburned surface category was not included as a potential suspended sediment source in the *upstream site* because of its small area (i.e. 19% of total catchment area) and its very limited hydrological connectivity with the stream network. This latter factor is due to the presence of well-maintained agricultural terraces (cf. Calsamiglia et al., 2017) and a road that isolates most of the unburned area (Fig. 1E), acting as an artificial longitudinal buffer against the fire and directing most runoff outside the catchment.

The catchment's hydrological dynamics between the wildfire and the sampling campaign resulted in the accumulation of 107 mm of low-intensity precipitation, which did not generate surface runoff at the catchment outlet (precipitation data from B118 S'Alqueria AEMET station, Fig. 1B). Visual evidence during the sampling campaign suggested incorporation of part of the ash deposits in the soil profile through infiltration (see ash cover in photos taken during the sampling campaign; Supplementary Fig. 1). For a few samples, the remaining ash cover was carefully removed to collect representative samples of the soil surface and minimise alteration of intrinsic soil properties.

Suspended sediment samples (n = 9) were collected during the hydrological years between 2013 and 2015 at both sampling sites (i.e. *upstream site* and *downstream site*), using time-integrated samplers (Phillips et al., 2000; two samplers per site). Ash was not collected at the study site. However, ash samples were collected from a fire-affected area in August 2018 in the municipality of Lluçmajor (southwest Mallorca; Fig. 1B). This burned site had similar soil types, climate and vegetation patterns. Representative ashes with a wide spectrum of colours (white, grey and black) were collected, avoiding the inclusion of the underlying soil layer (Bodí et al., 2014). In a simplified procedure, the samples were combined in two groups representing the overall gradient of ash colours, namely the black ashes (n = 10), i.e. the darker samples, and the grey ashes (n = 9), the lighter samples. Although the ash sampling area and the study area encompass similar characteristics, collecting ash samples in the study area just after the 2013 wildfire have been preferable. Thereby, even incorporating ashes with a large range of colours in the analysis, eventual difference between ashes from both sites remain unknown.

3.3. Laboratory treatment and analysis

The source and target sediment samples were oven-dried at 40 °C, disaggregated using a pestle and a mortar and sieved to < 63 µm to minimize the differences in particle size composition between source/target samples (Walling et al., 1993). The particle size distribution (PSD) and the specific surface area (SSA) of all source samples and 3 suspended sediment samples were determined after sieving by using a Malvern Mastersizer 2000 at the Institute of Environmental Assessment and Water Research (IDAEA-CSIC, Spain). The Shapiro-Wilk ($p < 0.05$) normality test and the Mann-Whitney *U* test checked the similarity in the PSD of each source group and target sample. ¹³⁷Cs and ²¹⁰Pb_{ex} activity concentrations (Bq·kg⁻¹) were measured by gamma spectrometry at the *Environmental Radioactivity Laboratory* of the University of the Balearic Islands (Mallorca, Spain), using a high-purity coaxial intrinsic germanium (HPGe) detector. Total C and N were measured by high-temperature combustion using a TruSpec CHNS, LECO at the Luxembourg Institute of Science and Technology (LIST, Luxembourg).

Diffuse reflectance was measured in a dark room by a spectroradiometer (ASD FieldSpect-II) at 1 µm steps over the 400–2500 µm range. The spectrometer was located in a tripod perpendicular to a flat surface, at 10 cm from the reference standard panel of known reflectivity (Spectralon). The soil and sediment samples were placed in transparent P.V.C. round petri dishes (4.7 cm diameter; Pall Corporation) and carefully smoothed with a spatula to minimize micro shadow effects due to surface roughness. The samples and the Spectralon were illuminated at an angle of 30° by a 50-w quartz halogen lamp placed at ca. 30 cm of distance. Following the International Commission on Illumination (CIE, 1931), CIE xyY colour coefficients were computed (i.e. cie x, cie y and cie yy) from the spectra reflectance measurements and the RGB colour values (i.e. red, green and blue). Then, the ColoSol software, developed by Viscarra Rossel et al. (2006), was used to estimate the Munsell HVC (i.e. Munsell H, Munsell V and Munsell C), CIE XYZ (i.e. cie X, cie Y and cie Z), CIE LAB (cie L, cie a* and cie b*), CIELUB (i.e. cie L, cie u* and cie v*), CIELHC (i.e. cie L, cie H and cie C) and decorrelated RGB (i.e. HRGB, IRGB and SRGB) colour parameters, as well as the redness index (i.e. RI) and Helmholtz chromaticity coordinates (i.e. DW nm, Pe %).

All the samples were placed in transparent plastic bags (7 * 5 cm) and scanned with an office scanner (Konika Minolta bizhub C554e; e.g. Krein et al., 2003; Pulley and Rowntree, 2016). The instrument was not calibrated. Red, green and blue colour parameters (i.e. RGB model) were extracted from the scanned images by the GIMP 2 open-source image-editing software. Then, the procedure described in the previous paragraph was applied to convert the red, green and blue colour parameters into the other colour parameters. This allowed us to

determine whether colour parameters calculated from diffuse reflectance (hereafter referred to as spectrometer-based colour parameters) and with an ordinary office scanner (hereafter referred to as scanner-based colour parameters) were consistent.

Ash exhaustion and soil recovery over time could alter source colour values, resulting in larger source ascription uncertainties in the medium to long term after the fire. However, sources were only sampled once (1 month after the fire). To partially mitigate this limitation, we made use of 24 soil samples collected in 2016 (29 months after the fire) from a headwater field on the study site (Fig. 1E). Samples were collected following the same methodology as in 2013 and scanned to measure their colour parameters. The samples were originally collected to analyse soil quality parameters after a wildfire (Calsamiglia et al., 2017; Lucas-Borja et al., 2018).

3.4. Artificial laboratory mixtures

Thirty artificial mixtures of 2, 3 and 4 different source samples, ash and suspended sediment were created (Table 1 and Supplementary Table 1). Mixtures of different sample types and a reduced number of mixtures with two or three samples of the same source were created. In the latter case, as all samples were considered as different sources, they permitted the uncertainty assessment when source tracer signatures were less distant. In addition, and to investigate ash influence on the colour parameters, 18 artificial samples mixing suspended sediment (collected at the *upstream site* in 2015) and ash (black and grey) in different proportions were created (Table 1 and Supplementary Table 2). The ash proportion was gradually modified from 10% to 90% to observe the influence of ash on sediment colour variation. Colour parameters of all the artificial mixtures were measured with the spectrometer and the scanner following the methodology described in Section 3.3.

3.5. Accuracy of colour tracers

The individual accuracy and linear additivity behaviour of colour tracers were assessed by comparing measured values (i.e. spectrometer- and colour-based ones) and predicted values by means of a mass balance approach (i.e. tracer values in the mixture are equal to the sum of contributions from each artificially mixed sample). To compare colour tracers with different scales, the normalized root mean square error (nRMSE) was calculated by dividing the RMSE by the mean of the measured data. The nRMSE was expressed as a percentage. The tracers with a nRMSE > 15% were discarded.

A Kruskal-Wallis H test was performed to find how well the colour tracers discriminated between source groups. Then, a Discriminant Function Analysis (DFA) checked the discriminatory potential of each tracer group (taking selected tracers as independent variables) and calculated the percentage of correctly classified samples (leave-on-out cross-validation).

3.6. Suspended sediment fingerprinting and unmixing of artificial mixtures

A range test was used to exclude potentially non-conservative tracers in each individual suspended sediment sample. Therefore, the tracers in suspended sediment and artificial mixtures that showed values outside minimum and maximum source range values were discarded.

The MixSIAR Bayesian tracer mixing model framework (Stock et al., 2018), implemented by Stock and Semmens (2016) as an open-source R package, was used to estimate the relative contribution of each source to the suspended sediment samples and the artificial mixtures. Previous studies using Bayesian mixing models to unmix sediment sources include Abbán et al., 2016; Blake et al., 2018; Massoudieh et al., 2013; and Nosrati et al., 2014.

The fundamental mixing equation of a mixing model is:

$$b_i = \sum_{j=1}^m w_j \cdot a_{i,j} \quad (1)$$

where b_i is the tracer property i ($i = 1$ to n) measured in a suspended sediment sample, $a_{i,j}$ is the value of the tracer property i in each source sample j ($j = 1$ to m), w_j is the unknown relative contribution of each source j to the suspended sediment sample. MixSIAR accounts for variability in the source and mixture tracer data with the ability to incorporate covariance data to explain variability in the mixture proportions via fixed and random effects (Stock and Semmens, 2016; Stock et al., 2018). This is especially useful in this study because of the collinearity between colour parameters of the different chromaticity coordinates. Hence, a discriminant function was not used to select an optimum group of tracers, as weak tracers can only improve model representation. In this study, MixSIAR was formulated by using sediment type as a factor and an uninformative prior (Blake et al., 2018). The Markov Chain Monte Carlo parameters were set as very long: chain length = 1,000,000, burn = 700,000, thin = 300, chains = 3. Convergence of the models was evaluated by the Gelman-Rubin diagnosis.

MixSIAR was used to unmix the artificial mixtures (see Section 3.4) and ultimately to evaluate and compare the performance of the two different colour tracer groups and FRNs. A constant residual error of 5% in the mixed samples was taken as creating the artificial mixtures to account for potential variability (e.g. measurement error). It should be noted that tracers that showed no individual discriminatory accuracy were excluded from the model (see Section 3.5). Accuracy in predicting the source contribution of each tracer group was evaluated by computing absolute errors (i.e. absolute value of the difference between the real proportions in the mixture and the estimated contributions; AE).

4. Results

4.1. Artificial laboratory mixtures and ash influence

Colour parameters showed individual contrasting performance to predict the colour of artificial mixtures (Fig. 2; Table 1). Chromatic coordinates *cie x* and *cie y* showed a maximum nRMSE between estimated and predicted values of 2% and 5% for the spectrometer-based (Fig. 2A and C) and scanner-based (Fig. 2B and D) parameters, respectively. Regardless of the measurement technique, *cie x* and *cie y* had lower nRMSE than red, green and blue colour parameters. In contrast, *cie yy* (brightness) had larger errors. The spectrometer-based *cie yy* parameter showed a minimum of 21% nRMSE (Fig. 2A); and the *cie yy* scanner-based one, a minimum of 15% (Fig. 2B). Thus, as *Cie yy* performance was low, it was not considered a linearly additive tracer. Fig. 2A and B also show that the divergence between estimated and measured *cie yy*, red, green and blue (i.e. nRMSE values) decreased when discarding one artificial mixture with black ash ($n = 9$; Fig. 2A and B). For instance, the average spectrometer- and scanner-based *cie yy*, red, green and blue nRMSEs decreased to 13%, 6%, 4% and 5%, respectively. Linear additivity tests were performed for all other spectrometer- and scanner-based colour parameters to discard non-linearly additive tracers. The remaining colour parameters were used to predict suspended sediment sources (Table 2).

The average nRMSE between estimated and predicted values was slightly higher for the 3-sample mixtures than for the 2-sample ones, for both the spectrometer- (4.2% higher) and the scanner-based (1.1% higher) colour parameters (Fig. 2). The 4-sample mixtures' average nRMSE was lower than the 2-sample mixtures' average nRMSE for both the spectrometer-based (1.3% lower) and the scanner-based (2.4% lower) colour parameters.

Accuracy of spectrometer- and scanner-based colour parameters was similar. Accordingly, colour parameters calculated using the two independent techniques correlated closely ($n = 24$; confidence limit 99%; $P < 0.01$) (see Supplementary Fig. 2). Despite this, the relationship between colour parameters calculated with the two techniques does not

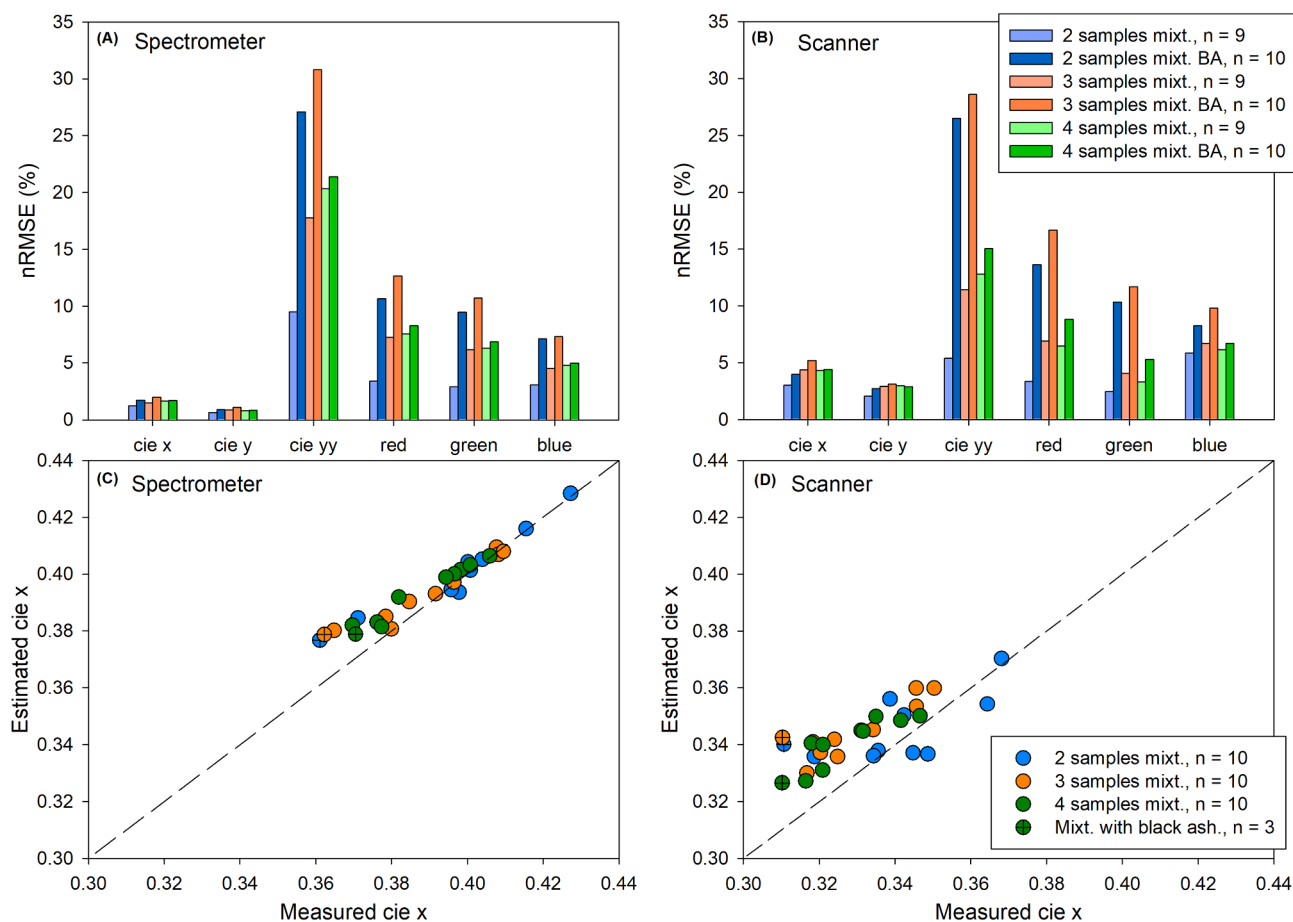


Fig. 2. Normalized root mean square error (nRMSE) between estimated and measured spectrometer-based (A) and scanner-based colour parameters (B). Note that nRMSE results are shown when including samples containing black ashes (BA; i.e. '2 samples mixt. BA', '3 samples mixt. BA' and '4 samples mixt. BA') and excluding them from the mixtures (i.e., '2 samples mixt.', '3 samples mixt.' and '4 samples mixt.'). Note that accuracy increase in the latest case. Scatter plot showing estimated versus measured *cie x* spectrometer-based parameter (C) and *cie x* scanner-based parameter (D) when mixing 2, 3 and 4 samples.

always follow the identity line.

Fig. 3 shows the estimated vs measured spectrometer-based colour parameters of the artificial sediment-ash mixtures (*cie x*, *cie y* and *cie yy*; Fig. 3A-C) and the nRMSE (*cie x*, *cie y*, *cie yy*, red, green and blue; Fig. 3D). Colour parameters changed clearly when regular proportions of ash were added to a suspended sediment sample (i.e., from 10 to 90%). For all colour parameters except green, the real measurements are over-estimated when a mass-balance approach is used (data not shown). *Cie x* and *cie y* parameters' nRMSE values were relatively low (i.e. < 3%) for both grey and black ash mixtures. However, *cie yy* showed a larger nRMSE (i.e. 10% for grey ash mixtures and 74% for black ash mixtures), confirming that it did not behave as a linearly additive tracer. The nRMSE values were higher on the RGB chromatic scale than on *cie x* and *cie y*. Mixtures with black ash showed larger errors than grey ash mixtures. Grey ash mixtures' nRMSEs for red, green and blue were < 10% (Fig. 3D). On the contrary, nRMSEs for black ash mixtures were > 10%. Errors were lower with a large contribution of one of the samples to the mixture (i.e. less deviation from the identity line in Fig. 3A-C), whereas errors increased if the proportion of both samples mixed was similar. In addition, and for comparison, analysis of the redness index evolution in black and grey artificial mixtures showed close positive correlation with $R^2 > 0.9$ in both cases (Fig. 3F and G).

In addition, increases in total C and total N were observed when the proportion of ash in the mixtures increased (Fig. 3H and I). On average, total C content increased by 0.6% and 6.4% for each 10% increase in grey and black ash content, respectively. Total N average increase was 0.01% and 0.04% for grey and black ash mixtures, respectively.

The MixSIAR Bayesian tracer mixing model framework was used to calculate the contribution of each sample to the artificial laboratory mixtures and to evaluate the overall unmixing performance of the colour tracers (using parameters showing a nRMSE < 15% on passing a range test for each mixture; unmixing results shown in Supplementary Tables 3–5 for 2, 3 and 4 samples mixed, respectively). MixSIAR predictions were compared with the real proportions mixed. The average absolute error when mixing 2, 3 and 4 samples ranged between 10.1 and 12.3% (Table 1). When unmixing 2 samples and one of the samples contributed more than 60% to the mixture, MixSIAR was able to identify the dominant sample in 4 of 6 cases. For 3-sample mixtures, MixSIAR was able to identify the dominant source in the 2 artificial samples when one of the samples contributed more than 60% to the mixture. Finally, when unmixing 4-sample mixtures, MixSIAR correctly identified the sample with a contribution > 40% to the mixture in 4 of 6 samples. In addition, some samples showed widespread distribution in the solutions of the model (e.g. mix2-m7), though the distribution did not include the real mixed sample proportion (e.g. mix2-m2).

4.2. Colour, particle size, organic matter content and FRN activity of sources, ash and suspended sediment samples

Samples collected at the downstream site from distinct sources had distinct colour values (Fig. 4; $p < 0.05$, K-Wallis test at 95% confidence interval; Supplementary Table 6). The unburned surface samples showed the highest values of all measured colour parameters, followed by the channel bank and the burned surface samples.

Table 1
Summary table of the type and number of artificial mixtures created in the laboratory. Average absolute error between real and estimated proportions using spectrometer-based colour parameter in MixSIAR. Real and estimated proportions of samples mixed are listed in Supplementary Tables 3, 4 and 5.

| Samples | Number of samples mixed (n-sources) | Number of mixtures (n) | Average absolute error (%) | Type of samples mixed |
|--------------------|-------------------------------------|------------------------|----------------------------|---|
| 2-samples mixtures | 2 | 10 | 12.3 | Channel bank, surface unburned, surface burned, grey ash, black ash |
| 3-samples mixtures | 3 | 10 | 12.3 | Channel bank, surface unburned, surface burned, grey ash, black ash |
| 4-samples mixtures | 4 | 10 | 10.1 | Channel bank, surface unburned, surface burned, grey ash, black ash |
| Black ash mixtures | 2 | 9 | - | Ash and suspended sediment |
| Grey ash mixtures | 2 | 9 | - | Ash and suspended sediment |

Suspended sediment colour measurements fall within the limits of the sources, with no evidence of missed sources seen. The values of suspended sediments were usually medium–low and similar to the values measured in the burned surface and channel bank samples. Black ash samples showed the lowest colour values. However, grey ash samples showed very low values for *cie x* and *cie y*, but notably higher values for *cie yy*.

At the downstream site, burned surface samples showed the highest redness index values, followed by channel banks and unburned surfaces (Fig. 5A). Accordingly, suspended sediment samples showed a higher redness index during the first event, which decreased over time at both sampling sites (Fig. 5B).

The discriminant function analysis showed that the selected spectrometer- and scanner-based parameters (Table 2) correctly classified 80% and 78.3% of the source samples, respectively, and that the selected tracers were able to distinguish sediment sources (Fig. 6).

Particle size distribution between source groups and suspended sediment samples was not normal (Shapiro-Wilk, $p < 0.05$). When applying the Mann-Whitney *U* test, all source sample groups showed statistical similarity with the suspended sediment samples (channel bank: $U = 2281$, $p = 0.894$; burned surface: $U = 2280$, $p = 0.890$; unburned surface: $U = 2267$, $p = 0.846$; Fig. 7).

Total C and N measured in source, suspended sediment and ash samples are shown in Fig. 8. Total C and N measured in suspended sediment and source samples showed significant inverse correlation with spectrometer-based *cie x* ($R = 0.71$ for both total C and N, $n = 67$, $p < 0.05$; Fig. 8) and *cie y* colour parameters ($R = 0.72$ and 0.77 , for total C and N, respectively, $n = 67$, $p < 0.05$; data not shown).

Suspended sediment samples from the *upstream* and *downstream sites* were collected for (i) two events occurring in the first post-fire hydrological year and (ii) two events in the second post-fire hydrological year (Fig. 9). Table 3 summarizes the hydrological and sediment transport dynamics of the events. It is of note that during the 29/10/2013 event, when precipitation intensity was ca. 5 times higher than the average of the rest of events, discharge and suspended sediment concentration peaks were an order of magnitude higher. At both sites, suspended sediment collected during the first event had the lowest colour values for *cie x*, *cie y* and *cie yy*, whereas values tended to increase in consecutive events (Table 3). However, it is the last event that shows the highest values at the *upstream site*. At the *downstream site*, the highest values were measured during the 15/12/2014 event, followed by the last event.

Burned surface samples showed the highest average activity values for ^{137}Cs and $^{210}\text{Pb}_{\text{ex}}$ (Table 4). Channel bank and unburned surface samples had very similar average FRN activities. These samples did not pass the K-Wallis distribution test ($p > 0.05$) and were grouped into a single source (i.e. referred to as unburned-channel).

Similar FRNs activities in unburned surface and channel bank samples can be explained as a consequence of a patchy fire effect within some streams. Flame turbulent processes can patchily influence the combustion in channel banks of intermittent streams, particularly considering those constrained by dry stone walls. However, some samples collected in unburned areas also showed high ^{137}Cs and $^{210}\text{Pb}_{\text{ex}}$ activities (supplementary Fig. 3A). The low energy conditions at the lower Sa Font de la Vila River (i.e. low gradient of the main channel) together with the dry conditions promoted sediment deposition in the mainstream. As most of the channel banks in this lowest reach were completely constrained by dry-stone walls, the samples were collected in the most bottom part of the channel banks. The sediment released from burned areas just after the first effective event (29th October 2013) were deposited within the channel bed and also affecting the bottom part of channel banks, thus promoting the increase of FRNs concentrations (supplementary Fig. 3B).

Both FRNs passed the K-Wallis test when two sources instead of three were considered: burned surface and unburned-channel. Suspended sediment samples' FRN values fell within the range of

Table 2
Tracers with a linear additivity behaviour.

| | Spectrometer-based parameters | Scanner-based parameters |
|------------------------------------|---|--|
| Linear additivity test: | | |
| Colour parameters with nRMSE < 15% | cie x, cie y, red, green, blue, HRGB, IRGB, cie L, cie H, Munsell H, Munsell V, DW nm, Pe % | cie x, cie y, green, blue, IRGB, cie L, Munsell V, DW nm |

activities measured on the sources.

4.3. Suspended sediment fingerprinting

All colour tracers that surpassed the linear additive test also passed the range test (spectrometer- and scanner-based colour parameters, Table 2) for the first two suspended sediment samples collected at the *upstream site* (i.e. US1 and US2). However, some colour parameters did not pass the test for the US3 samples (i.e. blue with scanner-based colour parameters) and US4 (green, blue, cie L, Munsell V with scanner and red, green, blue, IRGB, cie L, Munsell V with spectrometer-based colour parameters). For the suspended sediment samples collected at the *downstream site*, all tracers passing the linear additive test also passed the range test (spectrometer- and scanner-based colour parameters). Both ^{137}Cs and $^{210}\text{Pb}_{\text{ex}}$ passed the range test.

When using spectrometer-based colour parameters at the *upstream site*, mixing models predicted that burned soil contributed to the largest extent to the suspended sediment samples US1 and US2 (Table 5); whereas predictions for the US3 and US4 suspended sediment samples determined channel bank as the dominant source. At the *downstream site*, predicted suspended sediment sources changed over time. DS1a and DS1b were collected in parallel during the same event and predicted similar contributions (the first post-fire flush 29/10/2013). The mixing models predicted a dominant contribution of burned soil over the other sources (Table 5). The predominant source was still burned soil for the next sample collected (DS2), but the predicted predominant source changed towards unburned soil for the DS3 sample. Finally, for the DS4 sample, the mixing models predicted that the main suspended sediment source was again burned soil, followed by unburned soil.

When comparing the MixSIAR predictions obtained using different groups of tracers (i.e. spectrometer- and scanner-based colour parameters and FRNs), the three tracer groups predicted the same dominant source in all samples except three (US1, US2 and DS4; Table 5). When only comparing the spectrometer colour-based parameters and the FRN results, the two groups always identified the same dominant source (Table 5) except for the DS4 sample.

The source samples collected in 2016 showed scanner-based colour values that range between the burned soil and the unburned soil samples (Fig. 10A and B). To verify eventual ash exhaustion impact on our results, we determined suspended sediment sources by using MixSIAR and the colour parameters measured in the 2016 soil samples as burned sources (i.e. instead of the samples collected in 2013). The results did not substantially change, with an average absolute error of $5.7 \pm 6.6\%$ (Fig. 10B and C).

5. Discussion

5.1. On the use of colour to trace suspended sediment sources in burned Mediterranean catchments

The presence of ash after a wildfire tends to change the soil's visible reflectance (Lentile et al., 2006) and its carbon content (Bodí et al., 2014) and, in consequence, the colour of the upper soil layer. Results illustrated how colour parameters estimated from diffuse reflectance laboratory measurements discriminate between burned surface soil, unburned surface soil and channel bank sources. Artificial mixtures showed that most colour parameters were linear additive and,

individually, were able to predict the colour of the mixtures by using a mass balance approach. The highest errors were observed for the *cie yy*, SRGB, *cie X*, *cie Z*, *cie a**, *cie b**, *cie u**, *cie v**, *cie C*, Munsell C and redness index parameters (nRMSE > 15%). Therefore, they were discarded as reliable sediment tracers. Once the non-conservative tracers were discarded, the average nRMSE was equal to $5.1\% \pm 2.9$. Errors were comparable with values reported in the literature. Martínez-Carreras et al. (2010c) reported errors < 5% for 75% of their artificial mixtures using *cie x*, *cie y* and *cie yy* colour parameters, whilst the nRMSE ranged between 0.2 and 6.3% when 15 colour coefficients were used by Uber et al. (Uber et al., 2019) and between 0.4 and 5.6% by Gaspar et al. (2019) with geochemical tracers.

Furthermore, the presence of black ash in the artificial mixtures resulted in increased nRMSEs for some colour coefficients (e.g. *cie yy*; Fig. 2), suggesting that (i) these tracers should be discarded and (ii) colour tracers should be evaluated locally and carefully when source and sediment tracers contain black ashes. The differences in *cie yy* nRMSE obtained in artificial samples containing grey and black ashes may be due to different optical absorption. Black ashes had a lower reflectance with an average brightness (i.e. *cie yy*) of 2.8 ± 0.4 , while grey ashes showed an average of 17.3 ± 3.8 (spectrometer-based colour data). However, other parameters (e.g. *cie x* and *cie y*) were not significantly affected when black ash was added to the artificial mixtures (nRMSE always < 4%). These were the most reliable colour tracers.

Cie x and *cie y* values decreased when the ash proportion in the artificial mixtures increased (Fig. 3), whereas total C and N content increased. The average increase in the sediment total C content caused for each increase of 10% in the proportion of black ash is 10 times higher than for each increase of grey ash. Suspended sediment samples collected at the *upstream* and *downstream sites* and the grey ash sediment mixtures have similar proportions of C (i.e. ranging from 7.2 to 15.3%). However, even with similar total C content, the suspended sediment samples had higher *cie x* and *cie y* colour values than the grey ash artificial mixtures did (Fig. 11). This, together with the results of the mixing experiments, suggests that most of the suspended sediment samples contained < 20% of black ash (92.5% of the samples showed values higher than those of the samples containing 20% of black ash; Fig. 11) or < 30% of grey ash (Fig. 11). Thus, colour parameters can be used to calculate the ash content of soil and sediment samples. For instance, a gradual increase in the *cie x* and *cie y* colour values was observed in the suspended sediment samples collected at the *upstream* and *downstream sites* during subsequent events (Fig. 9), suggesting a decrease in their ash content. Likewise, Reneau et al. (2007) used ^{137}C activity to demonstrate that the proportion of ash in suspended sediment steadily decreased through the first rainy post-fire season and was lower in the second one.

The apparent decrease in ash content in suspended sediment samples over time (Fig. 11) could be associated, not only with a variation in the main source of sediment (i.e. burned surface), but also with ash exhaustion on the hillslopes. The latter is informed by the redness index, which correlates closely with the percentage of grey and black ash in the artificial mixtures (Fig. 3F and G). Hence, the ash experiments showed that the amount of ash also alters the redness index regardless of the temperature reached during the fire. Therefore, even if the redness index steadily decreases over time at both the *upstream* and *downstream sites* (Fig. 5B), it alone cannot confirm that there were

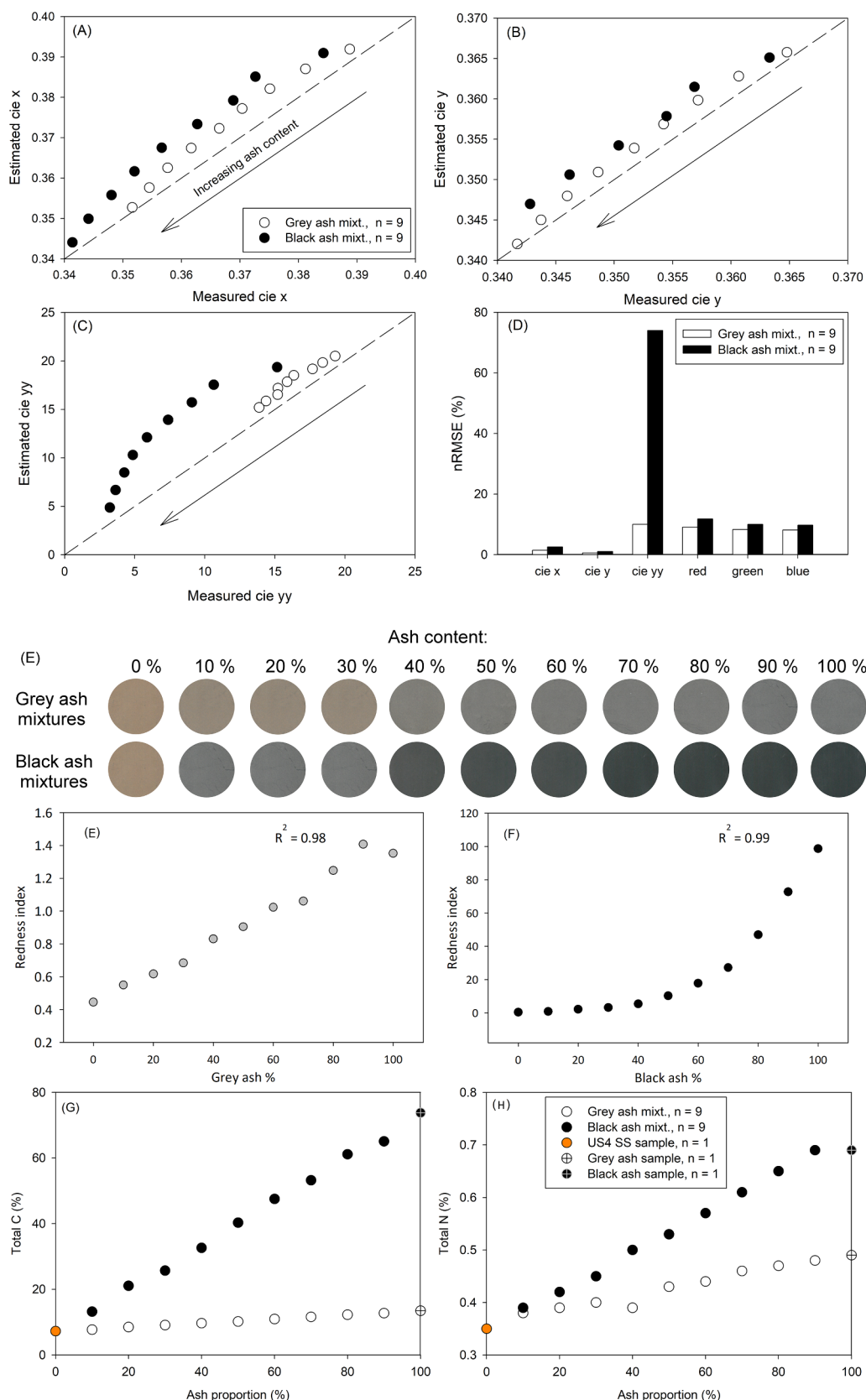


Fig. 3. Scatter plots showing estimated versus measured *cie x* (A), *cie y* (B) and *cie yy* (C) spectrometer-based colour parameter when adding increasing proportions of ash (black and grey ash; 0–100%) to a suspended sediment sample. (D) Normalized root mean square error (nRMSE) between estimated and measured spectrometer-based *cie x*, *cie y*, *cie yy*, red, green and blue colour parameters of the artificial sediment-ash mixtures. (E) Scanned images of the sediment-ash artificial mixtures when increasing the ash proportion (grey and black ash mixtures). (F) correlation between grey and (G) black ash % and redness index measured in the artificial mixtures. (H) scatter plot between total C and *cie x* and (I) between total N and *cie x* of the sediment-ash artificial mixtures, the US4 suspended sediment sample (US4 SS), and black and grey ash.

contributions from sources affected by fire, irrespective of the ash content in sediment.

Some studies report changes in the clay-sized material in sediments after a fire by the fusion of the finest particles, generating coarser

aggregates (Blake et al., 2007; Dyrness and Youngberg, 1957; Ternan and Neller, 1999). However, García-Corona et al. (2004) found no significant changes in aggregate size distribution in burned soils during a laboratory experiment. In this study, even if there were differences in

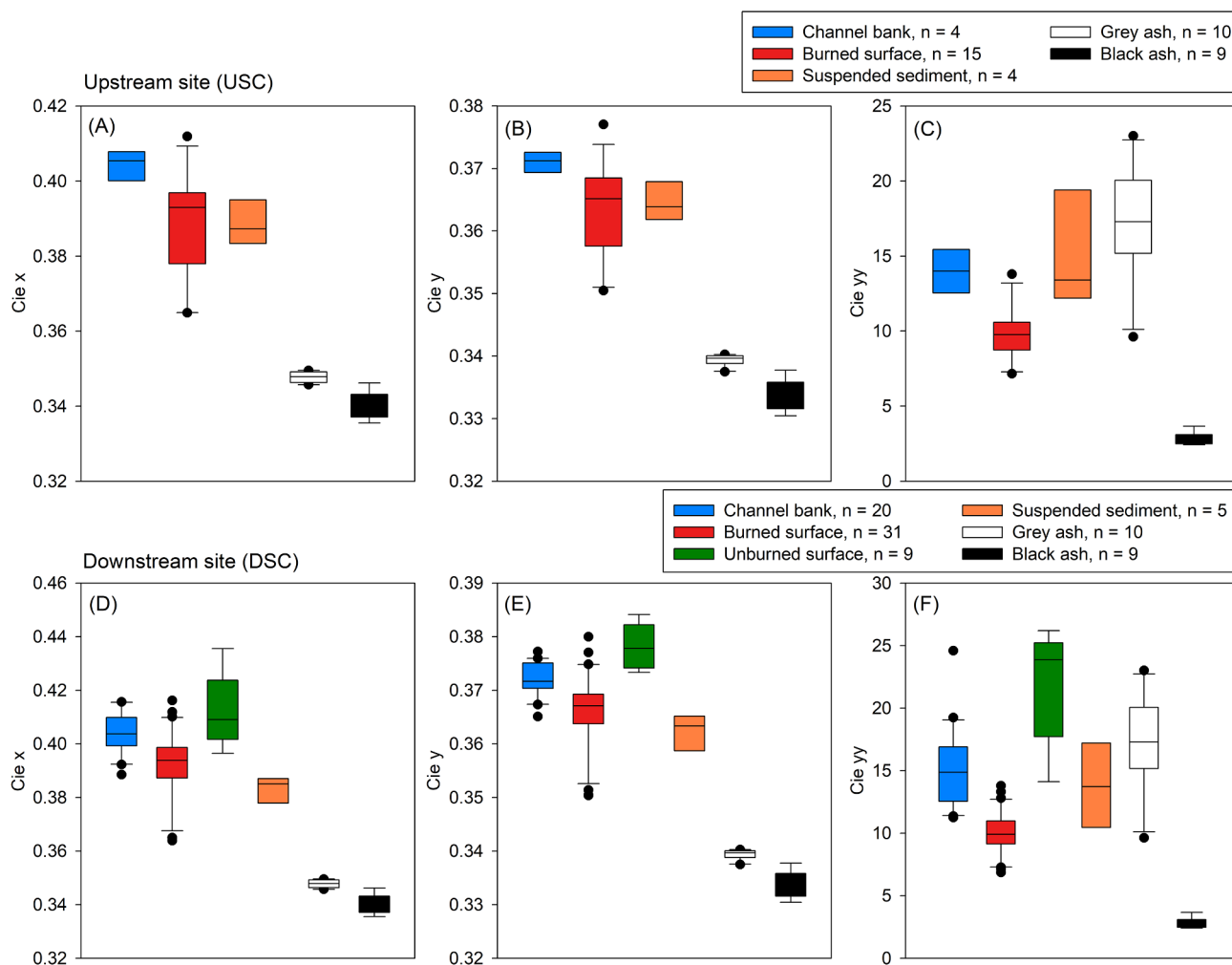


Fig. 4. Box plots of *cie x*, *cie y* and *cie yy* reflectance-based colour parameters measured in source and suspended sediment samples at the Sa Murtera sub-catchment (upstream site; A, B and C) and at the Font de la Vila catchment (downstream site; D, E and F). Values measured on grey and black ashes are plotted for comparison.

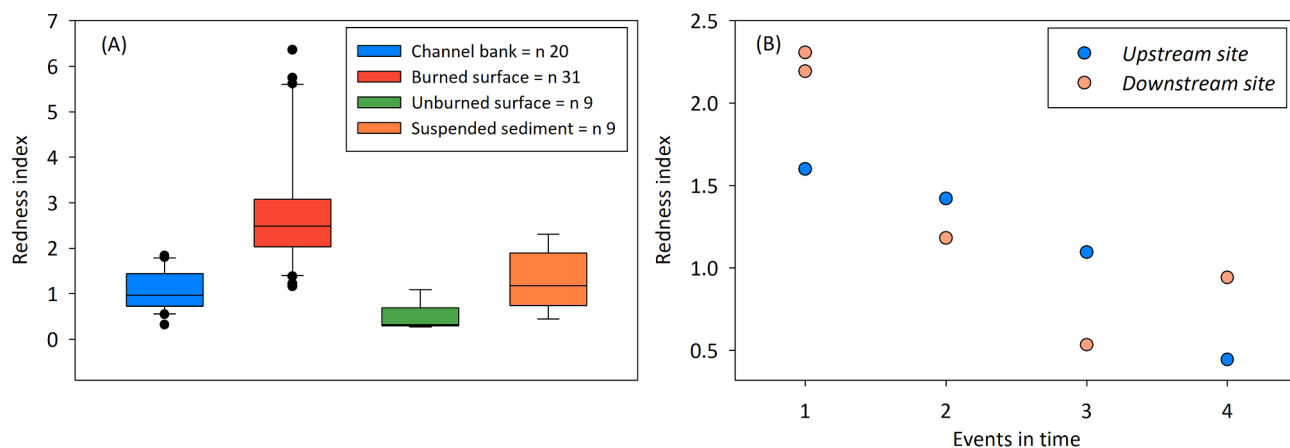


Fig. 5. (A) Boxplots showing the spectrometer-based redness index distribution values measured in sediment sources and suspended sediment samples from the downstream site; (B) evolution of the redness index values in suspended sediment samples trough time (x axis represents the chronological order of the events; see Table 3).

particle size distribution between suspended sediment and source samples (Fig. 5), they were not statistically significant. Nevertheless, samples were not sieved at different fractions and the influence of PSD on colour parameters was not addressed and should be further explored. Pulley and Rowntree (2016) found that the intensity of red,

green and blue light reflected from the < 32 μm fraction of the sediment was significantly higher than that of coarser particles (i.e. 63–32 μm and 125–63 μm fractions). When these authors, working in the Karoo region of the Eastern Cape of South Africa, separated the < 32 μm fraction of the sources and sediments from the > 32 μm fraction,

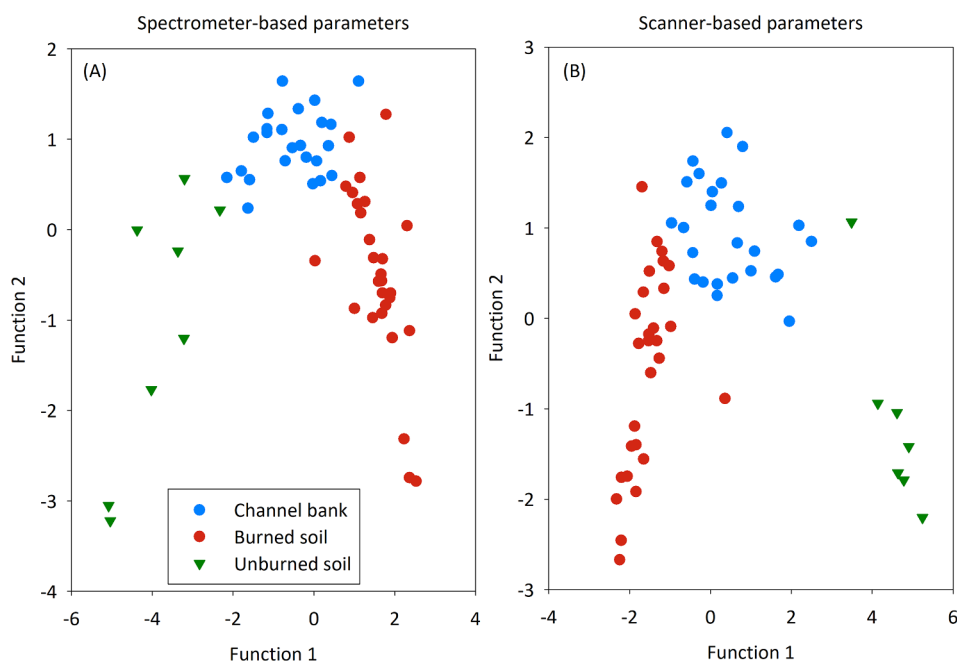


Fig. 6. Bi-plot showing the first and second discriminant functions for the spectrometer- (A) and scanner-based colour parameters (B) measured on the different source types of Sa Font de la Vila catchment (*downstream site*). Tracers used are listed in Table 2.

there was less tracing uncertainty. Even though the Karoo region covers a much larger area (> 150 km²) where in-stream transformations are more likely to occur than at our study site (< 5 km²), the extent of suspended sediment colour changes as a function of suspended sediment PSD and catchment size remains unknown and site-dependent.

Organic matter content also modifies the effectiveness of colour tracers to discriminate sediment sources if suspended sediment content increases during transport due to in-stream transformation. In non-burned catchments, Ankers et al. (2003) found C concentrations ranging from 4.5 to 12.2% in suspended sediment collected at 60 different catchments. In burned catchments, soil C content substantially increases when organic-rich ashes are incorporated into the soils at low combustion completeness (typically T < 450 °C), with organic C content as the main component (Bodí et al., 2014). However, lower C

content is expected in burned soils at high combustion completeness (typically T > 450 °C), as most organic carbon is volatilized. At our study site, the average total C content of burned soils was 2.3% higher than that of unburned soils, and 2.1% higher than in channel banks, which suggests the incorporation of low-combustion ashes. We argue that changes in total C content associated with ash incorporation and/or soil transformation after a wildfire, when low-combustion ashes are incorporated, are much larger than eventual changes due to in-stream transformation in small catchments. In this study, on average, total C increased by 0.6% ± 0.2 and 6.4% ± 2.5, respectively, when the proportion of grey and black ash in the artificial mixtures increased by 10% (Fig. 11). Pulley and Rowntree (2016) used H₂O₂ to remove organic matter in their South Africa samples to evaluate the uncertainties associated with organic matter when using colour to trace suspended

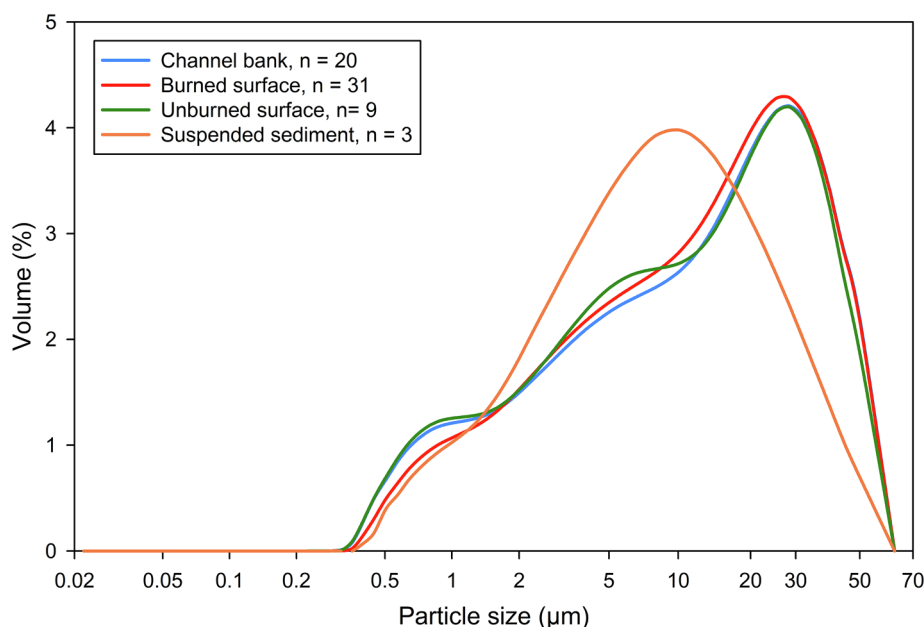


Fig. 7. Average particle size distributions of the different source types of Sa Font de la Vila catchment (*downstream site*) and suspended sediment samples.

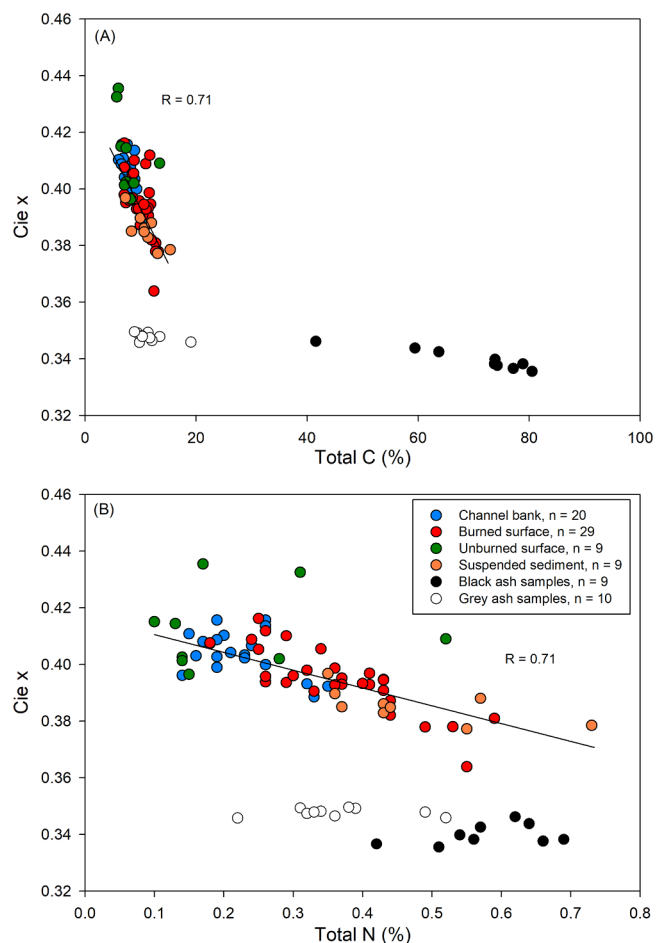


Fig. 8. Scatter plots between suspended sediment, source samples, black ash and grey ash chromatic coordinate $cie\ x$ and Total C (A), and Total N (B). R linear correlation coefficients for the source and sediment samples.

sediment sources. Their results showed that H_2O_2 treatment reduced source variability, homogenizing tracer values for each source and improving the discrimination capacity of colour tracers over untreated samples. However, the capacity of these tracers to discriminate between surface and subsurface sources was reduced. The authors also artificially added organic matter to some mixtures and observed that it had very little impact on the precision of colour tracers when it was < 30% of the sample mass. In later research, Pulley et al. (2018) detected that differences of 44% resulted when treating or not with H_2O_2 sediment and soil samples. When comparing these results with those provided by mineral magnetic tracers, the authors concluded that the errors were lower in the untreated samples, which means that the elimination of organic matter using H_2O_2 added more uncertainties to the unmixing process.

The capacity of colour tracers to unmix artificial laboratory mixtures was evaluated by the MixSIAR software. The results of our study illustrated average absolute errors of $12.3\% \pm 9.1$, $12.3\% \pm 4.2$ and $10.1\% \pm 4.2$ for 2-, 3- and 4-source mixtures, respectively. These errors were of the same order of magnitude as errors obtained by other authors using other tracers. Haddadchi et al. (2014) applied four different models using geochemical tracers to 20 artificial mixtures and obtained mean absolute errors ranging from 10.8% to 28.7%. Lower errors were found by Brosinsky et al. (2014), who used VNIR-SWIR spectral features to unmix 33 artificial samples and found errors < 10% in practically all cases. Gaspar et al. (2019) also obtained similar results with RMSEs ranging between 0.4% and 5.9% when they unmixed 12 artificial mixtures (10 replicas each) from 3 sets of different

geochemical tracers. Nevertheless, Uber et al. (2019) demonstrated, using three different mixing models (i.e. NNLS, SIMMR and PLSR), that the choice of tracers generates a greater impact on the model results than the type of model used. However, other authors found that different results might also be associated with the mixing models used (Haddadchi et al., 2014). In addition, if colour signatures are relatively similar (e.g. mix4-m4, mix4-m5, Supplementary Table 5), colour tracer measurements are not precise enough to quantify source contributions accurately.

Chromatic parameters calculated from the spectrometer in the laboratory and scanner-based colour parameters correlate closely ($p < 0.01$), which confirms that colour parameters provided by an office scanner are as reliable as colour tracers from a spectrophotometer. The differences in the absolute values obtained with the two techniques are related to (i) different measurement environments (i.e. dark room vs. office) and (ii) a lack of scanner calibration. Pulley and Rowntree (2016) demonstrated the reliability of an ordinary scanner in sediment fingerprinting research. They compared colour signatures with mineral magnetic signatures to trace bed and suspended sediment in the South African Karoo. The discriminatory efficiency of colour signatures ranged between 92.2% and 96.7% and were comparable to the results obtained using mineral magnetic signatures (i.e. 94%).

5.2. Suspended sediment origin after a wildfire in a Mediterranean catchment

The use of colour parameters to determine suspended sediment sources in the Sa Murtera (*upstream site*) and Sa Font de la Vila (*downstream site*) catchments, both affected by a wildfire in 2013, was assessed. Since errors associated with the unmixing of artificial samples might be high (see Section 5.1), the results using reflectance-based and scanner-based colour parameters were compared with those obtained using radioisotopes (i.e. ^{137}Cs and $^{210}Pb_{ex}$). It had been shown previously that the FRNs were able to recognize sediment sources in burned catchments (Wilkinson et al., 2009). The use of multi-fingerprint techniques is crucial to detect and quantify potential biases between different tracer sets and obtain reliable and robust estimates (e.g. Uber et al., 2019). In general, results showed that the three tracer groups predicted the same dominant source (Table 5). Nevertheless, at the *upstream site*, tracing results for the first two samples (i.e. US1 and US2) obtained with the scanner-based colour parameters indicated a different dominant source from the spectrometer-based colour parameters and the FRNs (Table 5). When looking at the tracer values' distribution measured for both samples and sources (Supplementary Fig. 4), we can see that both the spectrometer- and scanner-based colour parameters show $cie\ x$ and $cie\ y$ values similar to the values measured on burned surfaces. However, green and blue tracer values are similar to the values measured in channel banks. We argue that these differences are the main cause of divergence in the source ascription results. Furthermore, the small number of channel bank samples ($n = 4$) could misrepresent the real colour tracer variability of this source and confuse the un-mixing results. The results obtained with FRNs help us to determine the main suspended sediment source for the US1 sample (burned soil with an average contribution of 83.3 ± 12.3 , Table 5). However, FRNs showed poor discrimination for US2, which does not allow clear determination of the main suspended sediment source contributing to this sample. Nevertheless, the main predicted source for the 4 *upstream site* suspended sediment samples always coincides in both the spectrometer-based colour parameters and the radionuclides. However, the results for US2 (Table 5) are not very reliable because of the similar proportions of the two sources considered. At the *downstream site*, the main contributing source was the same for the three groups of tracers in all cases except for the 4th sample, in which scanner-based parameters and FRNs indicated dominance of the channel bank and unburned surface areas. The low suspended sediment

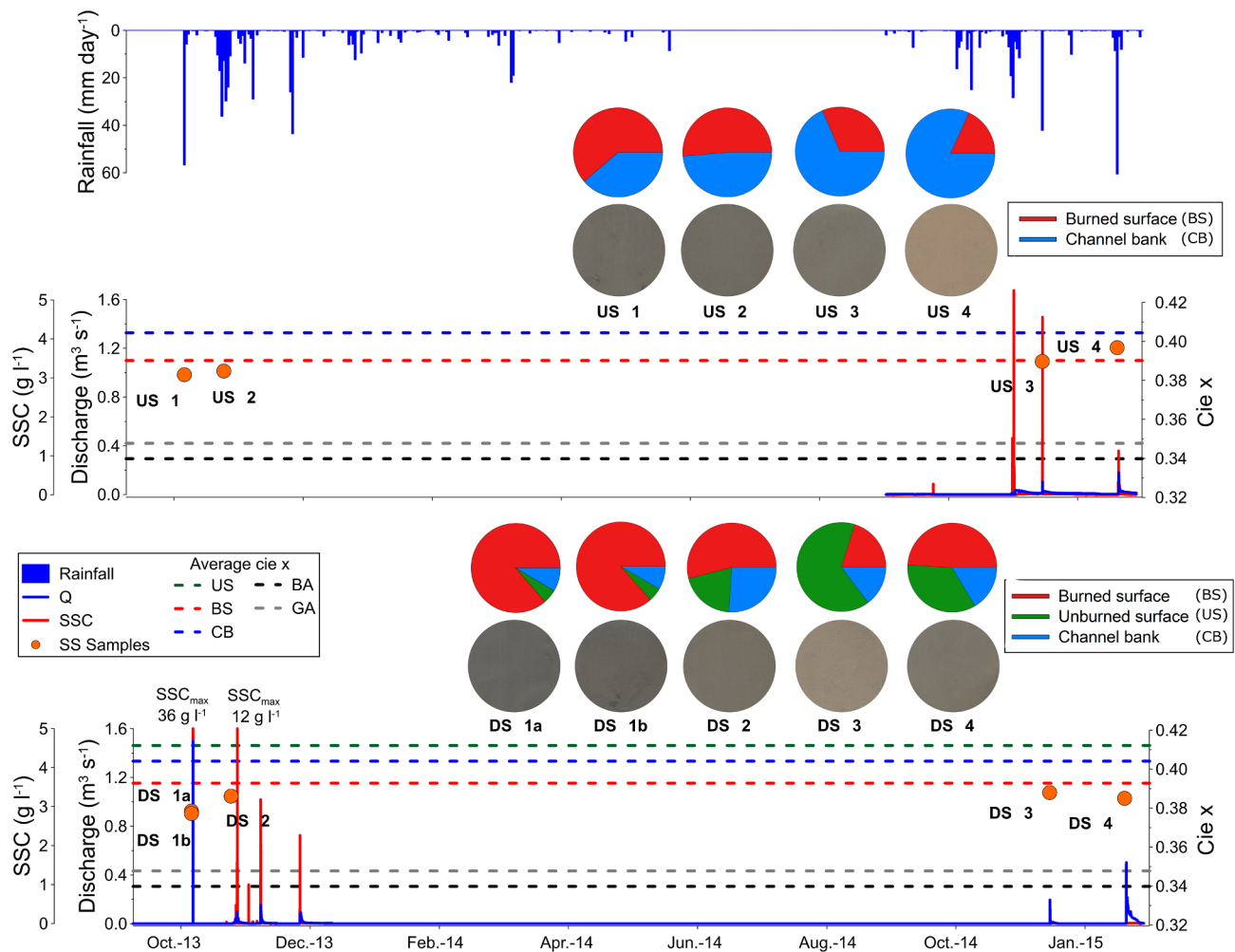


Fig. 9. Hydrograph, suspended sediment concentration (SSC) and hyetograph at the Sa Murtera sub-catchment (middle plot; *upstream site*) and the Sa Font de la Vila catchment (lower plot; *downstream site*) during the study period. Average *Cie x* colour parameter values for each potential suspended sediment sources type (unburned surface (US), burned surface (BS) and channel bank (CB), grey and black ashes (GA and BA, respectively) represented as dotted lines. *Cie x* colour parameter values measured on the suspended sediment (SS) samples represented as orange dots. Pie charts show suspended sediment average source ascription at both sampling sites together with a picture of the suspended sediment collected with the time-integrated sampler during each event.

concentration peak and the delivered load during the 4th event (Table 3) may indicate not only a low slope-to-channel sediment mobilization, but also the activation of small or very specific sediment sources not well represented in the sampling. Limitations in the technique to identify sediment sources at low suspended sediment concentrations could be involved during these low magnitude events.

Nevertheless, at both sites, results indicate that sediment contribution from burned surface sources dominated the first hydrological year, whereas unburned surface and channel banks dominated the second hydrological year.

The samples collected in 2016 were used to validate the hypothesis that some ash remained in the burned soils two years after the fire.

Table 3

List of events sampled in the *upstream site* (Sa Murtera) and *downstream site* (Sa Font de la Vila). Total rainfall (P.tot.); maximum rainfall intensity in 30 min (IPmax-30); total sediment load (Load); maximum sediment concentration (SS peak), and the *Cie x*, *Cie y* and *Cie yy* spectrometer-based colour parameters measured in the suspended sediment samples. DS1a and DS1b were sampled simultaneously in the same event.

| Site | SS Samples | Date | P.tot. (mm) | IPmax-30 (mm·h ⁻¹) | Q peak (m ³ ·s ⁻¹) | Load (t) | SS peak (mg·l ⁻¹) | Colour parameters | | |
|------------------------|------------|------------|----------------|-----------------------------------|--|-------------|----------------------------------|-------------------|--------------|---------------|
| | | | | | | | | <i>Cie x</i> | <i>Cie y</i> | <i>Cie yy</i> |
| <i>Upstream site</i> | US1 | 29/10/2013 | 51 | 100 | – | – | – | 0.3829 | 0.3617 | 12.0399 |
| | US2 | 17/11/2013 | 66 | 18 | – | – | – | 0.3848 | 0.3624 | 12.6789 |
| | US3 | 15/12/2014 | 30 | 29.6 | 0.1 | 0.8 | 4.557 | 0.3897 | 0.3654 | 14.1313 |
| | US4 | 20/01/2015 | 62 | 10.8 | 0.2 | 0.7 | 11.245 | 0.3968 | 0.3687 | 21.1625 |
| <i>Downstream site</i> | DS1a* | 29/10/2013 | 51 | 100 | 1.5 | 84 | 36.030 | 0.3785 | 0.3592 | 10.5616 |
| | DS1b* | 29/10/2013 | 51 | 100 | 1.5 | 84 | 36.030 | 0.3772 | 0.3582 | 10.3677 |
| | DS2 | 17/11/2013 | 66 | 18 | 0.1 | 3 | 11.848 | 0.3861 | 0.3633 | 13.7114 |
| | DS3 | 15/12/2014 | 30 | 29.6 | 0.2 | 0.1 | 215 | 0.388 | 0.3665 | 19.3448 |
| | DS4 | 20/01/2015 | 62 | 10.8 | 0.5 | 1.1 | 285 | 0.3851 | 0.3639 | 15.0774 |

* Samples DS1a and DS1b were collected during the same event using two time-integrated suspended sediment samplers.

Table 4
Average Fallout radionuclide (FRNs) activity (Bq kg⁻¹) in the different source and sediment sample groups.

| Tracers | Sample groups | Mean (Bq kg ⁻¹) | Sta.Dev. |
|---------------------------------|--------------------|-----------------------------|----------|
| ²¹⁰ Pb _{ex} | Channel bank | 46.377 | 40.814 |
| | Burned surface | 204.138 | 98.312 |
| | Unburned surface | 42.045 | 52.376 |
| | Suspended sediment | 177.835 | 102.389 |
| ¹³⁷ Cs | Channel bank | 6.260 | 3.803 |
| | Burned surface | 28.665 | 16.076 |
| | Unburned surface | 5.811 | 6.118 |
| | Suspended sediment | 20.800 | 8.754 |

Thus, source samples collected after the fire were representative of the entire sediment sampling period. The *cie x*, *cie y* and RGB scanner-based colour value distribution (Fig. 10A and B) suggested that, although there were colour changes after the fire, most probably due to ash wash, there was still ash influence in the soil colour parameters. Furthermore, sediment ascription results in both 2013 and 2016 burned surface samples (Fig. 10B and C) were similar. Even if the changes in soil colour properties caused by the fire still prevail today in some areas, the samples collected in 2016 are not representative of the entire catchment (see Section 3.2 for details). Catchment-wide representative sampling would have been needed to improve the robustness of the source ascription results for the 2014 and 2015 suspended sediment samples.

In this study, it is assumed that sediment and ash were transported in association on their way from the hillslopes to the stream and remained in association during eventual deposition. However, this was not investigated. Direct observations indicated that water flows are notably turbulent at the study sites, generating a relatively homogeneous mixture of suspended sediment within the water column.

Table 5

MixSIAR source apportionment using spectrometer-based colour parameters, scanner-based colour parameters and fallout radionuclides activity (FRNs) for the suspended sediment samples collected at the *upstream* and *downstream* sites. It should be note that unburned surface and channel bank sources were joined for FRNs at the *downstream* site.

| SS sample | Sources | Spectrometer | | Scanner | | FRNs | |
|------------------------|------------------|--------------------|------------------------------------|--------------------|------------------------------------|--------------------|------------------------------------|
| | | Average (%) | Quantile distribution 2.5% – 97.5% | Average (%) | Quantile distribution 2.5% – 97.5% | Average (%) | Quantile distribution 2.5% – 97.5% |
| <i>Upstream site</i> | | | | | | | |
| US1 | Burned surface | 61.3 ± 10.3 | 43.5–83.9 | 39 ± 10.4 | 21.3–66.2 | 83.3 ± 12.3 | 52.2–99.3 |
| | Channel bank | 38.7 ± 10.3 | 16.1–56.5 | 61 ± 10.4 | 37.8–78.7 | 16.7 ± 12.3 | 0.7–44.8 |
| US2 | Burned surface | 51.4 ± 9.1 | 36.1–71.9 | 31.6 ± 12.3 | 8.3–58.4 | 55.1 ± 20.3 | 20.4–96.1 |
| | Channel bank | 48.6 ± 9.1 | 28.1–63.9 | 68.4 ± 12.3 | 41.6–91.7 | 44.9 ± 20.3 | 3.9–79.6 |
| US3 | Burned surface | 31.4 ± 9.4 | 11.7–50.1 | 8 ± 8.7 | 0.2–29.2 | 27.9 ± 19.5 | 2.5–80.3 |
| | Channel bank | 68.6 ± 9.4 | 49.9–88.3 | 92 ± 8.7 | 70.8–99.8 | 72.1 ± 19.5 | 19.7–97.5 |
| US4 | Burned surface | 18.1 ± 11.2 | 1.2–43.7 | 21.2 ± 2.2 | 0.6–85.8 | 21.3 ± 18.8 | 0.9–75.5 |
| | Channel bank | 81.9 ± 11.2 | 56.3–98.8 | 78.8 ± 2.2 | 14.2–99.4 | 78.7 ± 18.8 | 24.5–99.1 |
| <i>Downstream site</i> | | | | | | | |
| DS1a | Burned surface | 84.6 ± 6.4 | 70.9–96 | 88.4 ± 5.7 | 75.2–97.5 | 85.8 ± 10.3 | 62.4–99.5 |
| | Unburned surface | 5.7 ± 4.2 | 0.3–15.9 | 4.4 ± 3.4 | 0.2–12.8 | 14.2 ± 10.3 | 0.5–37.6 |
| DS1b | Channel bank | 9.7 ± 6.8 | 0.4–25.5 | 7.2 ± 5.8 | 0.2–21.8 | | |
| | Burned surface | 86.2 ± 6.1 | 73.3–96.7 | 81.3 ± 7.5 | 65.3–94.8 | 70.3 ± 16 | 40–97.8 |
| DS2 | Unburned surface | 5.1 ± 3.9 | 0.2–14.6 | 6.5 ± 4.7 | 0.3–17.2 | 29.7 ± 16 | 2.2–60 |
| | Channel bank | 8.7 ± 6.2 | 0.4–23 | 12.2 ± 8.4 | 0.5–30.4 | | |
| DS3 | Burned surface | 53.8 ± 8.7 | 36.8–70.3 | 53 ± 10.2 | 31.7–70.9 | 72.7 ± 15.3 | 43.5–98.1 |
| | Unburned surface | 19.8 ± 10 | 1.6–38 | 19 ± 10 | 1.4–38.1 | 27.3 ± 15.3 | 1.9–56.5 |
| DS4 | Channel bank | 26.4 ± 15.7 | 1.9–58.3 | 27.9 ± 17.2 | 1.4–63.1 | | |
| | Burned surface | 20.3 ± 9.5 | 2.1–38.2 | 8.6 ± 7.1 | 0.2–26 | – | – |
| DS4 | Unburned surface | 65 ± 10.5 | 45–84.2 | 65.9 ± 17.4 | 21.2–91.3 | – | – |
| | Channel bank | 14.7 ± 12.9 | 0.5–44.9 | 25.4 ± 20 | 1–75.1 | | |
| DS4 | Burned surface | 49 ± 7.9 | 32.7–63.3 | 28.4 ± 15.4 | 3–56.5 | 38.4 ± 19.8 | 7.9–86.4 |
| | Unburned surface | 34.4 ± 9.7 | 9.8–50.4 | 19.6 ± 16.2 | 0.5–52 | 61.6 ± 19.8 | 13.6–92.1 |
| | Channel bank | 16.6 ± 13.8 | 0.6–52.9 | 52.1 ± 29.1 | 1.6–91.8 | | |

Nevertheless, the sediment originating at unburned areas could be influenced by the ash during in-stream transport, generating erroneous source ascription results. Many authors have documented increased erosion rates, runoff coefficients and sediment delivery in burned areas (e.g. Shakesby and Doer, 2006; Vieira et al., 2015). In addition, the incorporation of ash to runoff tends to increase its density, resulting in greater erosivity potential and enhancing its sediment transport capacity (Gabet and Sternberg, 2008). Even so, the transport mechanisms of ash and mineral particles should be further explored to determine whether they are transported together and what influence they have on colour parameters. This would improve the robustness of the technique.

The main sediment sources in a burned catchment may vary according to catchment characteristics and the magnitude of post-fire rainfall events. Other studies of burned catchments also found temporal variations of the main sources of sediment. Distinguishing only between surface vs. subsurface sources and using radionuclides, Wilkinson et al. (2009) and Smith et al. (2011b) observed predominance of surface soil in two burned forested catchments in Australia, despite differences in fire severity patterns, size and geology characteristics. In addition, Smith et al. (2011b) found a gradual decrease of surface soil contributions during the first 4 years after the wildfire. However, Owens et al. (2012) found a predominance of subsurface/channel bank contributions in a semi-arid forested burned catchment in Canada, due to the low-intensity rainfall that constrained sediment delivery from hillslopes. Estrany et al. (2016) used radionuclides to trace suspended sediment sources after a wildfire in a small Mediterranean catchment in Spain. The authors also quantified a small contribution from burned areas (12% on average) to bed-sediment samples during a flood event characterised by 69 mm of total rainfall in 24 h.

Studies show divergences in landscape response after a wildfire. Predominant factors influencing erosive processes in burned

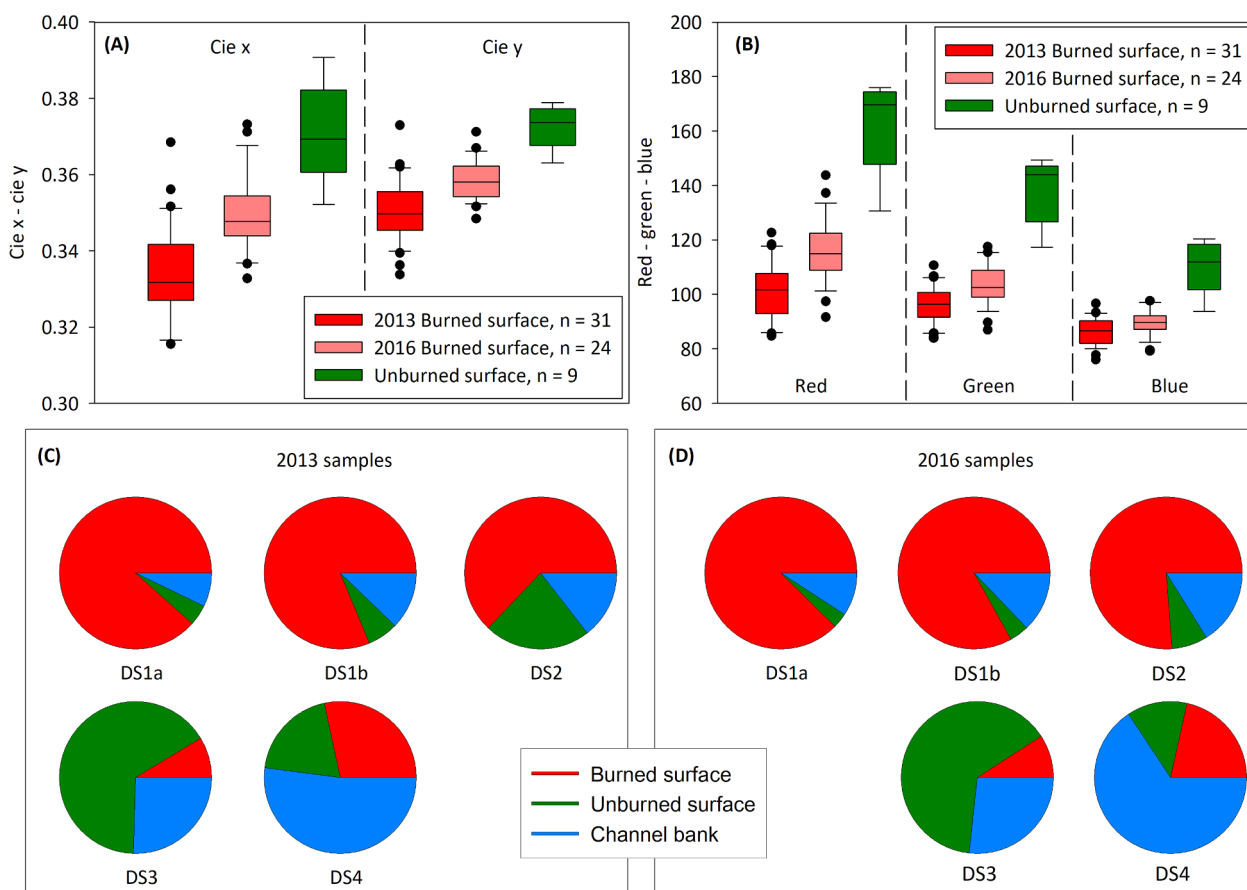


Fig. 10. (A) Box plots of *cie x* and *cie y* scanner-based colour parameters measured in 2013 burned source samples, 2016 burned source samples and 2013 unburned source samples; (B) Box plots of red, green, blue scanner-based colour parameters measured in 2013 burned source samples, 2016 burned source samples and 2013 unburned source samples; (C) Average MixSIAR source apportionment results using 2013 burned surface scanner-based colour parameters; (D) Average MixSIAR source apportionment results using 2016 burned surface scanner-based colour parameters.

catchments, besides fire, are the magnitude, frequency and intensity of post-fire rainfall and any associated floods (Moody and Martin, 2009; Smith et al., 2011ab). The Mediterranean is a highly energetic environment with large inter-annual variability of rainfall, resulting in different sediment yields and sediment origin depending on seasonality, preceding wetness conditions and intrinsic characteristics of each event. In addition, the important presence of agricultural terraces in the Sa Font de la Vila catchment (Fig. 1D) plays an important role in sediment connectivity, by decreasing water and sediment yield (Calsamiglia et al., 2018). García-Comendador et al. (2017a) analysed the hydrological dynamics and suspended sediment transport in the catchment during the first three post-fire years (2013–2016). The hysteresis analysis during this period concluded that 67% of the counter-clockwise hysteresis (i.e. associated with distant sediment sources, potentially burned areas in this case) occurred during the first year after the fire, decreasing significantly in subsequent years together with sediment yield. During these three years, 92% of the sediment was exported during the first event (October 2013; samples US1, DS1a and DS1b). These results corroborate the tracing results obtained with the spectrometer-based colour tracers, showing a decrease over time in the contribution from distant areas (i.e. fire-affected hillslopes) and variations in the main sediment sources over time (Table 5). The decrease in the sediment contribution from burned hillslopes is related not only to partial vegetation recovery, but also to that rainfall events occurring during the second year after the fire did not exceed the intensity thresholds needed to generate effective slope-to-channel connectivity (Calvo-Cases et al., 2003), resulting in disconnected burned hillslopes.

6. Conclusions

Colour tracers measured with a spectrometer and a scanner discriminate usefully between burned and unburned sediment sources. This is a result of the soil colour changes associated with the transformation of biomass, necromass and soil organic matter into ash during a fire. Colour parameters can be used in unmixing approaches to tracing suspended sediment sources after wildfires in small Mediterranean catchments, as our results are consistent – for most of the samples – with tracing results obtained with well-established radionuclides. The main advantage of colour parameters is that they can be measured quickly and are cheap and non-destructive. Hence, they enable post-fire management strategies to be decided quickly and their success to be followed up easily.

Nevertheless, results obtained using colour parameters must be carefully considered and cross-checked by use of other tracers. This might be even more important in burned catchments, where ash exhaustion and soil recovery during the disturbance period may affect colour parameters. Accordingly, variations in organic matter content and differences in particle size distribution need to be addressed.

In the Sa Font de la Vila catchment, the contribution of burned hillslopes to suspended sediment gradually decreased. We hypothesise that this might be related to partial vegetation recovery. However, it appears that the relatively low rainfall intensities measured during the second year after the fire might not have reached the thresholds for generating effective slope-to-channel connectivity. Further research is necessary to evaluate the recovery of the catchment, a highly variable and changing ecosystem.

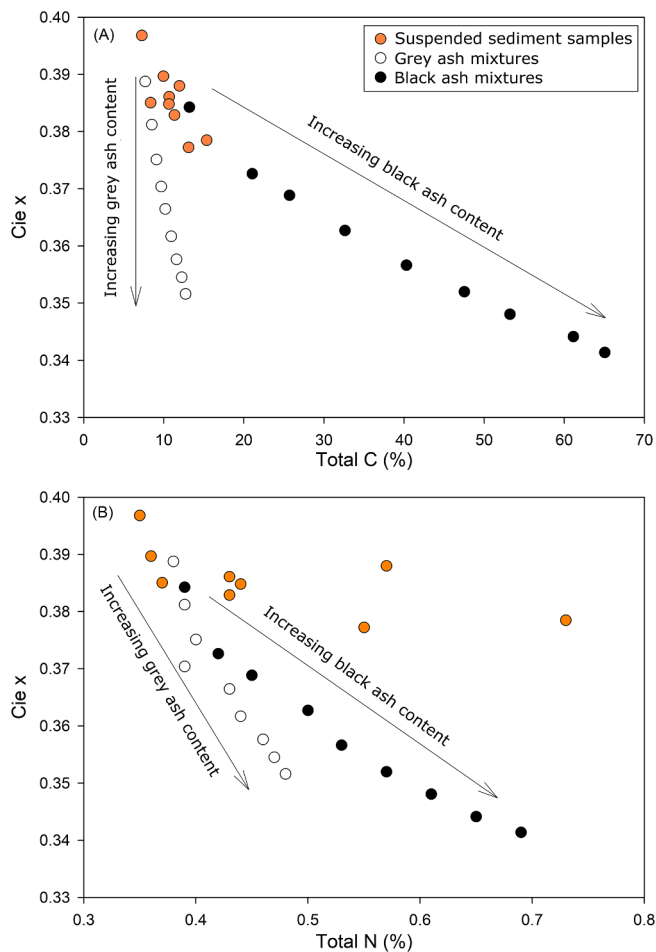


Fig. 11. Scatter plots showing suspended sediment samples, grey ash and sediment artificial mixtures and black ash and sediment artificial mixtures relationship of $cie x$ values and Total C (A), and Total N (B). Arrows indicate ash content increase in the artificial mixtures.

Finally, the lack of standardized protocols for sampling sediment sources in burned catchments should not be forgotten. The values of not only soil colour parameters, but also other tracers, change on the incorporation of ashes. Therefore, the sampling protocol (e.g. incorporating the layer of ash partially or completely removing it to reach the soil surface) and the sampling time (e.g. immediately after the fire or a few days later) require further research. The use of a standardized sampling method will allow better comparison between studies of different sites, as it would take into account not only the fire and the characteristics of the study area, but also post-fire hydrometeorological conditions.

Declaration of Competing Interest

The authors declare that they have no known competing financial interests or personal relationships that could have appeared to influence the work reported in this paper.

Acknowledgments

This research was supported by the Spanish Ministry of Science, Innovation and Universities, the Spanish Agency of Research (AEI) and the European Regional Development Funds (ERDF) through the project CGL2017-88200-R “Functional hydrological and sediment connectivity at Mediterranean catchments: global change scenarios –MEDhyCON2”. Julián García-Comendador is in receipt of a pre-doctoral contract

(FPU15/05239) funded by the Spanish Ministry of Education and Culture. Núria Martínez-Carreras acknowledges funding for this study from the Luxembourg National Research Fund (PAINLESS project, C17/SR/11699372). Josep Fortesa has a contract funded by the Vice-presidency and Ministry of Innovation, Research and Tourism of the Autonomous Government of the Balearic Islands (FPI/2048/2017). The contribution of Aleix Calsamiglia was supported by the Spanish Ministry of Science, Innovation and Universities through the pre-doctoral contract BES-2013-062887. Meteorological data were provided by the Spanish Meteorological Agency (AEMET). We would like to acknowledge support by François Barnich and Franz Kai Ronellenfitsch for the carbon and nitrogen measurements, and set-up of the spectroradiometer, respectively. We would like to also acknowledge the fundamental contribution of the reviewers in improving our manuscript.

Appendix A. Supplementary data

Supplementary data to this article can be found online at <https://doi.org/10.1016/j.geoderma.2020.114638>.

References

- Abban, B., Thanos Papanicolaou, A.N., Cowles, M.K., Wilson, C.G., Abaci, O., Wacha, K., Schilling, K., Schnoebelen, D., 2016. An enhanced Bayesian fingerprinting framework for studying sediment source dynamics in intensively managed landscapes. *Water Resour. Res.* 52, 4646–4673. <https://doi.org/10.1002/2015WR018030>.
- Ankers, C., Walling, D.E., Smith, R.P., 2003. The influence of catchment characteristics on suspended sediment properties. *Hydrobiologia* 494, 159–167. <https://doi.org/10.1023/A:1025458114068>.
- Balfour, V.N., Woods, S.W., 2013. The hydrological properties and the effects of hydration on vegetative ash from the Northern Rockies, USA. *Catena* 111, 9–24. <https://doi.org/10.1016/j.catena.2013.06.014>.
- Bauzá, J., 2014. Els grans incendis forestals a les Illes Balears: una resposta des de la teledetecció. Bachelor Thesis. University of the Balearic Islands, Palma, Spain.
- Blake, W.H., Boeckx, P., Stock, B.C., Smith, H.G., Bodé, S., Upadhayay, H.R., Gaspar, L., Goddard, R., Lennard, A.T., Lizaga, I., Lobb, D.A., Owens, P.N., Peticrew, E.L., Kuzyk, Z.Z.A., Gari, B.D., Munishi, L., Mtei, K., Nebiyu, A., Mabit, L., Navas, A., Semmens, B.X., 2018. A deconvolutional Bayesian mixing model approach for river basin sediment source apportionment. *Sci. Rep.* 8, 1–12. <https://doi.org/10.1038/s41598-018-30905-9>.
- Blake, W.H., Droppo, I.G., Humphreys, G.S., Doerr, S.H., Shakesby, R.A., Wallbrink, P.J., 2007. Structural characteristics and behavior of fire-modified soil aggregates. *J. Geophys. Res.* Earth Surf. 112, F02020. <https://doi.org/10.1029/2006JF000660>.
- Bodí, M.B., Martín, D.A., Balfour, V.N., Santín, C., Doerr, S.H., Pereira, P., Cerdà, A., Mataix-Solera, J., 2014. Wildland fire ash: production, composition and eco-hydro-geomorphic effects. *Earth-Science Rev.* 130, 103–127. <https://doi.org/10.1016/j.earscirev.2013.12.007>.
- Brook, A., Wittenberg, L., Kopel, D., Polinova, M., Roberts, D., Ichoku, C., Shtober-Zisu, N., 2018. Structural heterogeneity of vegetation fire ash. *L. Degrad. Dev.* 29, 2208–2221. <https://doi.org/10.1002/ldr.2922>.
- Brosinsky, A., Foerster, S., Segl, K., Kaufmann, H., 2014. Spectral fingerprinting: sediment source discrimination and contribution modelling of artificial mixtures based on VNIR-SWIR spectral properties. *J. Soils Sediments* 14, 1949–1964. <https://doi.org/10.1007/s11368-014-0925-1>.
- Calsamiglia, Aleix, Fortesa, Josep, García-Comendador, Julián, Lucas-Borja, Manuel E., Calvo-Cases, Adolfo, Estrany, Joan, 2018. Spatial patterns of sediment connectivity in terraced lands: Anthropogenic controls of catchment sensitivity. *Land Degrad. Dev.* 29 (4), 1198–1210. <https://doi.org/10.1002/ldr.2840>.
- Calsamiglia, A., Lucas-Borja, M.E., Fortesa, J., García-Comendador, J., Estrany, J., Calsamiglia, A., Lucas-Borja, M.E., Fortesa, J., García-Comendador, J., Estrany, J., 2017. Changes in soil quality and hydrological connectivity caused by the abandonment of terraces in a mediterranean burned catchment. *Forests* 8, 333. <https://doi.org/10.3390/f8090333>.
- Calvo-Cases, A., Boix-Fayos, C., Imeson, A.C., 2003. Runoff generation, sediment movement and soil water behaviour on calcareous (limestone) slopes of some Mediterranean environments in southeast Spain. *Geomorphology* 50, 269–291. [https://doi.org/10.1016/S0169-555X\(02\)00218-0](https://doi.org/10.1016/S0169-555X(02)00218-0).
- Candela, A., Aronica, G., Santoro, M., 2005. Effects of Forest Fires on Flood Frequency Curves in a Mediterranean Catchment/Effets d'incendies de forêt sur les courbes de fréquence de crue dans un bassin versant Méditerranéen. *Hydrol. Sci. J.* 50, 206. <https://doi.org/10.1623/hysj.50.2.193.61795>.
- Cerdà, A., Doerr, S.H., 2008. The effect of ash and needle cover on surface runoff and erosion in the immediate post-fire period. *Catena* 74, 256–263. <https://doi.org/10.1016/J.CATENA.2008.03.010>.
- Collins, A.L.L., Pulley, S., Foster, I.D.L.D.L., Gellis, A., Porto, P., Horowitz, A.J.J., 2017. Sediment source fingerprinting as an aid to catchment management: a review of the current state of knowledge and a methodological decision-tree for end-users. *J. Environ. Manage.* 194, 86–108. <https://doi.org/10.1016/j.jenvman.2016.09.075>.
- D'Haen, K., Duser, B., Verstraeten, G., Degryse, P., De Brue, H., 2013. A sediment

- fingerprinting approach to understand the geomorphic coupling in an eastern Mediterranean mountainous river catchment. *Geomorphology* 197, 64–75. <https://doi.org/10.1016/j.geomorph.2013.04.038>.
- Davis, C.M., Fox, J.F., 2009. Sediment fingerprinting: review of the method and future improvements for allocating nonpoint source pollution. *J. Environ. Eng.* 135, 490–504. [https://doi.org/10.1061/\(ASCE\)0733-9372\(2009\)135:7\(490\)](https://doi.org/10.1061/(ASCE)0733-9372(2009)135:7(490)).
- Dyrness, C.T., Youngberg, C.T., 1957. The effect of logging and slash-burning on soil structure. *Soil Sci. Soc. Am. J.* 21, 444–447. <https://doi.org/10.2136/sssaj1957.03615995002100040022x>.
- Escuin, S., Navarro, R., Fernández, P., 2008. Fire severity assessment by using NBR (Normalized Burn Ratio) and NDVI (Normalized Difference Vegetation Index) derived from LANDSAT TM/ETM images. *Int. J. Remote Sens.* 29, 1053–1073. <https://doi.org/10.1080/01431160701281072>.
- Estrany, J., López-Tarazón, J.A., Smith, H.G., 2016. Wildfire effects on suspended sediment delivery quantified using fallout radionuclide tracers in a mediterranean catchment. *L. Degrad. Dev.* 27, 1501–1512. <https://doi.org/10.1002/ldr.2462>.
- Evrard, O., Durand, R., Foucher, A., Tiecher, T., Sellier, V., Onda, Y., Lefèvre, L., Cerdan, O., Lacey, J.P., 2019. Using spectrocolourimetry to trace sediment source dynamics in coastal catchments draining the main Fukushima radioactive pollution plume (2011–2017). *J. Soils Sediments* 19, 3290–3301. <https://doi.org/10.1007/s11368-019-02302-w>.
- Gabet, E.J., Sternberg, P., 2008. The effects of vegetative ash on infiltration capacity, sediment transport, and the generation of progressively bulked debris flows. *Geomorphology* 101, 666–673. <https://doi.org/10.1016/j.geomorph.2008.03.005>.
- García-Comendador, J., Fortesa, J., Calsamiglia, A., Calvo-Cases, A., Estrany, J., 2017a. Post-fire hydrological response and suspended sediment transport of a terraced Mediterranean catchment. *Earth Surf. Process. Landforms* 42, 2254–2265. <https://doi.org/10.1002/esp.4181>.
- García-Comendador, J., Fortesa, J., Calsamiglia, A., Garcias, F., Estrany, J., 2017b. Source ascription in bed sediments of a Mediterranean temporary stream after the first post-fire flush. *J. Soils Sediments* 17, 2582–2595. <https://doi.org/10.1007/s11368-017-1806-1>.
- García-Corona, R., Benito, E., De Blas, E., Varela, M.E., 2004. Effects of heating on some soil physical properties related to its hydrological behaviour in two north-western Spanish soils. *Int. J. Wildl. Fire* 13, 195–199. <https://doi.org/10.1071/WF03068>.
- Gaspar, L., Blake, W.H., Smith, H.G., Lizaga, I., Navas, A., 2019. Testing the sensitivity of a multivariate mixing model using geochemical fingerprints with artificial mixtures. *Geoderma* 337, 498–510. <https://doi.org/10.1016/j.geoderma.2018.10.005>.
- Guijarro, J.A., 1986. *Contribucion a la bioclimatología de Baleares*. PhD Thesis. University of the Balearic Islands, Palma, Spain.
- Haddadchi, A., Olley, J., Lacey, P., 2014. Accuracy of mixing models in predicting sediment source contributions. *Sci. Total Environ.* 497–498, 139–152. <https://doi.org/10.1016/j.scitotenv.2014.07.105>.
- Horowitz, A.J., Elrick, K.A., Smith, J.J., 2007. Measuring the fluxes of suspended sediment, trace elements and nutrients for the city of atlanta, USA: Insights on the global water quality impacts of increasing urbanization. *IAHS-AISH Publ.* 314, 57–70.
- Jahn, R., Blume, H.P., Asio, V.B., Spaargaren, O., Schad, P., 2006. Guidelines for soil description, FAO. ed. Rome.
- Keeley, J.E., 2009. Fire intensity, fire severity and burn severity: a brief review and suggested usage. *Int. J. Wildl. Fire* 18, 116–126. <https://doi.org/10.1071/WF07049>.
- Ketterings, Q.M., Bigham, J.M., 2000. Soil Color as an Indicator of Slash-and-Burn Fire Severity and Soil Fertility in Sumatra, Indonesia. *Soil Sci. Soc. Am. J.* 64, 1826–1833. <https://doi.org/10.2136/sssaj2000.6451826x>.
- Krein, A., Petticrew, E., Udelhoven, T., 2003. The use of fine sediment fractal dimensions and colour to determine sediment sources in a small watershed. *Catena* 53, 165–179. [https://doi.org/10.1016/S0341-8162\(03\)00021-3](https://doi.org/10.1016/S0341-8162(03)00021-3).
- Lees, J.A., 1997. Mineral magnetic properties of mixtures of environmental and synthetic materials: linear additivity and interaction effects. *Geophys. J. Int.* 131, 335–346. <https://doi.org/10.1111/j.1365-246X.1997.tb01226.x>.
- Lentile, L.B., Holden, Z.A., Smith, A.M.S., Falkowski, M.J., Hudak, A.T., Morgan, P., Lewis, S.A., Gessler, P.E., Benson, N.C., 2006. Remote sensing techniques to assess active fire characteristics and post-fire effects. *Int. J. Wildl. Fire* 15, 319–345. <https://doi.org/10.1071/WF05097>.
- Lucas-Borja, M.E., Calsamiglia, A., Fortesa, J., García-Comendador, J., Lozano Guardiola, E., García-Orenes, F., Gago, J., Estrany, J., 2018. The role of wildfire on soil quality in abandoned terraces of three Mediterranean micro-catchments. *Catena* 170, 246–256. <https://doi.org/10.1016/j.catena.2018.06.014>.
- Martínez-Carreras, N., Krein, A., Gallart, F., Iffly, J.F., Pfister, L., Hoffmann, L., Owens, P.N., 2010a. Assessment of different colour parameters for discriminating potential suspended sediment sources and provenance: a multi-scale study in Luxembourg. *Geomorphology* 118, 118–129. <https://doi.org/10.1016/j.geomorph.2009.12.013>.
- Martínez-Carreras, N., Krein, A., Udelhoven, T., Gallart, F., Iffly, J.F., Hoffmann, L., Pfister, L., Walling, D.E., 2010b. A rapid spectral-reflectance-based fingerprinting approach for documenting suspended sediment sources during storm runoff events. *J. Soils Sediments* 10, 400–413. <https://doi.org/10.1007/s11368-009-0162-1>.
- Martínez-Carreras, N., Udelhoven, T., Krein, A., Gallart, F., Iffly, J.F., Ziebel, J., Hoffmann, L., Pfister, L., Walling, D.E., 2010c. The use of sediment colour measured by diffuse reflectance spectrometry to determine sediment sources: application to the Attert River catchment (Luxembourg). *J. Hydrol.* 382, 49–63. <https://doi.org/10.1016/j.jhydrol.2009.12.017>.
- Massoudieh, A., Gellis, A., Banks, W.S., Wiczorek, M.E., 2013. Suspended sediment source apportionment in Chesapeake Bay watershed using Bayesian chemical mass balance receptor modeling. *Hydro. Process.* 27, 3363–3374. <https://doi.org/10.1002/hyp.9429>.
- Moody, J.A., Martin, D.A., 2009. Synthesis of sediment yields after wildland fire in different rainfall regimes in the western United States. *Int. J. Wildl. Fire* 18, 96–115. <https://doi.org/10.1071/WF07162>.
- Moody, J.A., Shakesby, R.A., Robichaud, P.R., Cannon, S.H., Martin, D. a., 2013. Current research issues related to post-wildfire runoff and erosion processes. *Earth-Science Rev.* 122, 10–37. <https://doi.org/10.1016/j.earscirev.2013.03.004>.
- Navas, A., Garcés, B.V., Machín, J., 2004. An approach to integrated assessment of reservoir siltation: the Joaquín Costa reservoir as a case study. *Hydro. Easrt Syst. Sci.* 8, 1193–1199. <https://doi.org/10.5194/hess-8-1193-2004>.
- Newcombe, C.P., Macdonald, D.D., 1991. Effects of suspended sediments on aquatic ecosystems. *North Am. J. Fish. Manag.* 11, 72–82. [https://doi.org/10.1577/1548-8675\(1991\)011<0072:EOSSOA>2.3.CO;2](https://doi.org/10.1577/1548-8675(1991)011<0072:EOSSOA>2.3.CO;2).
- Nosrati, K., Govers, G., Semmens, B.X., Ward, E.J., 2014. A mixing model to incorporate uncertainty in sediment fingerprinting. *Geoderma* 217–218, 173–180. <https://doi.org/10.1016/j.geoderma.2013.12.002>.
- Nyman, P., Sheridan, G.J., Smith, H.G., Lane, P.N.J., 2014. Modeling the effects of surface storage, macropore flow and water repellency on infiltration after wildfire. *J. Hydrol.* 513, 301–313. <https://doi.org/10.1016/j.jhydrol.2014.02.044>.
- Owens, P.N., Blake, W.H., Giles, T.R., Williams, N.D., 2012. Determining the effects of wildfire on sediment sources using ¹³⁷Cs and unsupported ²¹⁰Pb: the role of landscape disturbances and driving forces. *J. Soils Sediments* 12, 982–994. <https://doi.org/10.1007/s11368-012-0497-x>.
- Pereira, P., Cerdà, A., Úbeda, X., Mataix-Solera, J., Arcenegui, V., Zavala, L.M., 2015. Modelling the impacts of wildfire on ash thickness in a short-term period. *L. Degrad. Dev.* 26, 180–192. <https://doi.org/10.1002/ldr.2195>.
- Pérez-Bejarano, A., Guerrero, C., 2018. Near infrared spectroscopy to quantify the temperature reached in burned soils: importance of calibration set variability. *Geoderma* 326, 133–143. <https://doi.org/10.1016/j.geoderma.2018.03.038>.
- Phillips, J.M., Russell, M.A., Walling, D.E., 2000. Time-integrated sampling of fluvial suspended sediment: a simple methodology for small catchments. *Hydro. Process.* 14, 2589–2602. [https://doi.org/10.1002/1099-1085\(20001015\)14:14<2589::AID-HYP94>3.0.CO;2-D](https://doi.org/10.1002/1099-1085(20001015)14:14<2589::AID-HYP94>3.0.CO;2-D).
- Pulley, S., Rowntree, K., 2016. The use of an ordinary colour scanner to fingerprint sediment sources in the South African Karoo. *J. Environ. Manage.* 165, 253–262. <https://doi.org/10.1016/j.jenvman.2015.09.037>.
- Pulley, S., Van der Waal, B., Rowntree, K., Collins, A.L., 2018. Colour as reliable tracer to identify the sources of historically deposited flood bench sediment in the Transkei, South Africa: a comparison with mineral magnetic tracers before and after hydrogen peroxide pre-treatment. *Catena* 160, 242–251. <https://doi.org/10.1016/j.catena.2017.09.018>.
- Reneau, S.L., Katzman, D., Kuyumjian, G.A., Lavine, A., Malmon, D.V., 2007. Sediment delivery after a wildfire. *Geology* 35, 151–154. <https://doi.org/10.1130/G23288A.1>.
- Scott, D., Versfeld, D.B., Lesch, W., 1998. Erosion and sediment yield in relation to afforestation and fire in the mountains of the western cape province, south africa. *South African Geogr. J.* 80, 52–59. <https://doi.org/10.1080/03736245.1998.9713644>.
- Shakesby, R.A. a., 2011. Post-wildfire soil erosion in the Mediterranean: Review and future research directions. *Earth-Science Rev.* 105, 71–100. <https://doi.org/10.1016/j.earscirev.2011.01.001>.
- Shakesby, R.A. a., Doerr, S.H.H., 2006. Wildfire as a hydrological and geomorphological agent. *Earth-Science Rev.* 74, 269–307. <https://doi.org/10.1016/j.earscirev.2005.10.006>.
- Smith, A.M.S., Wooster, M.J., Drake, N.A., Dipotso, F.M., Falkowski, M.J., Hudak, A.T., 2005. Testing the potential of multi-spectral remote sensing for retrospectively estimating fire severity in African Savannas. *Remote Sens. Environ.* 97, 92–115. <https://doi.org/10.1016/j.rse.2005.04.014>.
- Smith, H.G., Blake, W.H., 2014. Sediment fingerprinting in agricultural catchments: a critical re-examination of source discrimination and data corrections. *Geomorphology* 204, 177–191. <https://doi.org/10.1016/j.geomorph.2013.08.003>.
- Smith, H.G., Blake, W.H., Owens, P.N., 2013. Discriminating fine sediment sources and the application of sediment tracers in burned catchments: a review. *Hydro. Process.* 27, 943–958. <https://doi.org/10.1002/hyp.9537>.
- Smith, H.G., Sheridan, G.J., Lane, P.N.J., Nyman, P., Haydon, S., 2011a. Wildfire effects on water quality in forest catchments: a review with implications for water supply. *J. Hydrol.* 396, 170–192. <https://doi.org/10.1016/j.jhydrol.2010.10.043>.
- Smith, H.G., Sheridan, G.J., Lane, P.N.J., Noske, P.J., Hejnis, H., 2011b. Changes to sediment sources following wildfire in a forested upland catchment, southeastern Australia. *Hydro. Process.* 25, 2878–2889. <https://doi.org/10.1002/hyp.8050>.
- Spanos, I., Raftoyannis, Y., Goudelis, G., Xanthopoulou, E., Samara, T., Tsiotis, A., 2005. Effects of postfire logging on soil and vegetation recovery in a Pinus halepensis Mill. Forest of Greece. In: *Plant and Soil*. Kluwer Academic Publishers, pp. 171–179. <https://doi.org/10.1007/s11104-005-0807-9>.
- Stock, B., Semmens, B., 2016. MixSIAR GUI User Manual v3.1. <https://doi.org/10.5281/ZENODO.47719>.
- Stock, B.C., Jackson, A.L., Ward, E.J., Parnell, A.C., Phillips, D.L., Semmens, B.X., 2018. Analyzing mixing systems using a new generation of Bayesian tracer mixing models. *PeerJ* 6, e5096. <https://doi.org/10.7717/peerj.5096>.
- Terefe, T., Mariscal-Sancho, I., Peregrina, F., Espejo, R., 2008. Influence of heating on various properties of six Mediterranean soils. A laboratory study. *Geoderma* 143, 273–280. <https://doi.org/10.1016/j.geoderma.2007.11.018>.
- Ternan, J.L., Neller, R., 1999. The erodibility of soils beneath wildfire prone grasslands in the humid tropics, Hong Kong. *Catena* 36, 49–64. [https://doi.org/10.1016/S0341-8162\(99\)00011-9](https://doi.org/10.1016/S0341-8162(99)00011-9).
- Tiecher, T., Caner, L., Minella, J.P.G., dos Santos, D.R., 2015. Combining visible-based-color parameters and geochemical tracers to improve sediment source discrimination and apportionment. *Sci. Total Environ.* 527–528, 135–149. <https://doi.org/10.1016/j.scitotenv.2015.04.103>.
- Úbeda, X., Outeiro, L., 2009. Physical and chemical effects of fire on soil. In: Cerdà, A., Robichaud, P. (Eds.), *Fire Effects on Soils and Restoration Strategies*. Science

- Publishers, New Hampshire, pp. 105–132.
- Úbeda, X., Pereira, P., Outeiro, L., Martin, D.A., 2009. Effects of fire temperature on the physical and chemical characteristics of the ash from two plots of Cork oak (*Quercus Suber*). *L. Degrad. Dev.* 20, 589–608. <https://doi.org/10.1002/ldr.930>.
- Uber, M., Legout, C., Nord, G., Crouzet, C., Demory, F., Poulenard, J., 2019. Comparing alternative tracing measurements and mixing models to fingerprint suspended sediment sources in a mesoscale Mediterranean catchment. *J. Soils Sediments* 19, 3255–3273. <https://doi.org/10.1007/s11368-019-02270-1>.
- Verkaik, I., Vila-Escalé, M., Rieradevall, M., Prat, N., 2013. Seasonal drought plays a stronger role than wildfire in shaping macroinvertebrate communities of Mediterranean streams. *Int. Rev. Hydrobiol.* 98, 271–283. <https://doi.org/10.1002/iroh.201201618>.
- Vieira, D.C.S., Fernández, C., Vega, J. a., Keizer, J.J., 2015. Does soil burn severity affect the post-fire runoff and interrill erosion response? A review based on meta-analysis of field rainfall simulation data. *J. Hydrol.* 523, 452–464. <https://doi.org/10.1016/j.jhydrol.2015.01.071>.
- Viscarra Rossel, R.A., Minasny, B., Roudier, P., McBratney, A.B., 2006. Colour space models for soil science. *Geoderma* 133, 320–337. <https://doi.org/10.1016/J.GEODERMA.2005.07.017>.
- Walling, D.E., 2013. The evolution of sediment source fingerprinting investigations in fluvial systems. *J. Soils Sediments* 13, 1658–1675. <https://doi.org/10.1007/s11368-013-0767-2>.
- Walling, D.W., Woodward, J.C., Nicholas, A.P., 1993. A multi-parameter approach to fingerprinting suspended-sediment sources. *Tracers Hydrol. Proc. Int. Symp. Yokohama 1993*, 329–338.
- Warrick, J.A., Hatten, J.A., Pasternack, G.B., Gray, A.B., Goni, M.A., Wheatcroft, R.A., 2012. The effects of wildfire on the sediment yield of a coastal California watershed. *Bull. Geol. Soc. Am.* 124, 1130–1146. <https://doi.org/10.1130/B30451.1>.
- Wilkinson, S.N.N., Wallbrink, P.J.J., Hancock, G.J.J., Blake, W.H.H., Shakesby, R.A.A., Doerr, S.H.H., 2009. Fallout radionuclide tracers identify a switch in sediment sources and transport-limited sediment yield following wildfire in a eucalypt forest. *Geomorphology* 110, 140–151. <https://doi.org/10.1016/J.GEOMORPH.2009.04.001>.